Supporting Information

Pyridine-driven assembly of Zn(II) and Cd(II) complexes with 2-furoic acid. The role of water in a structural transformation

Daniel Ejarque [a], *Francisco Sánchez-Férez* [a], *Núria Félez-Guerrero* [a], *Teresa Calvet* [b], *Mercè Font-Bardia* [c], *and Josefina Pons* [a,*]

[a]Departament de Química, Universitat Autònoma de Barcelona, 08193-Bellaterra, Barcelona, Spain

[b]Departament de Mineralogia, Petrologia i Geologia Aplicada, Universitat de Barcelona, Martí i Franquès s/n, 08028 Barcelona, Spain

[c]Unitat de Difracció de Raig-X, Centres Científics i Tecnològics de la Universitat de Barcelona (CCiTUB), Universitat de Barcelona, Solé i Sabarís, 1-3, 08028 Barcelona, Spain

*Corresponding author E-mail: josefina.pons@uab.es

PXRD patterns

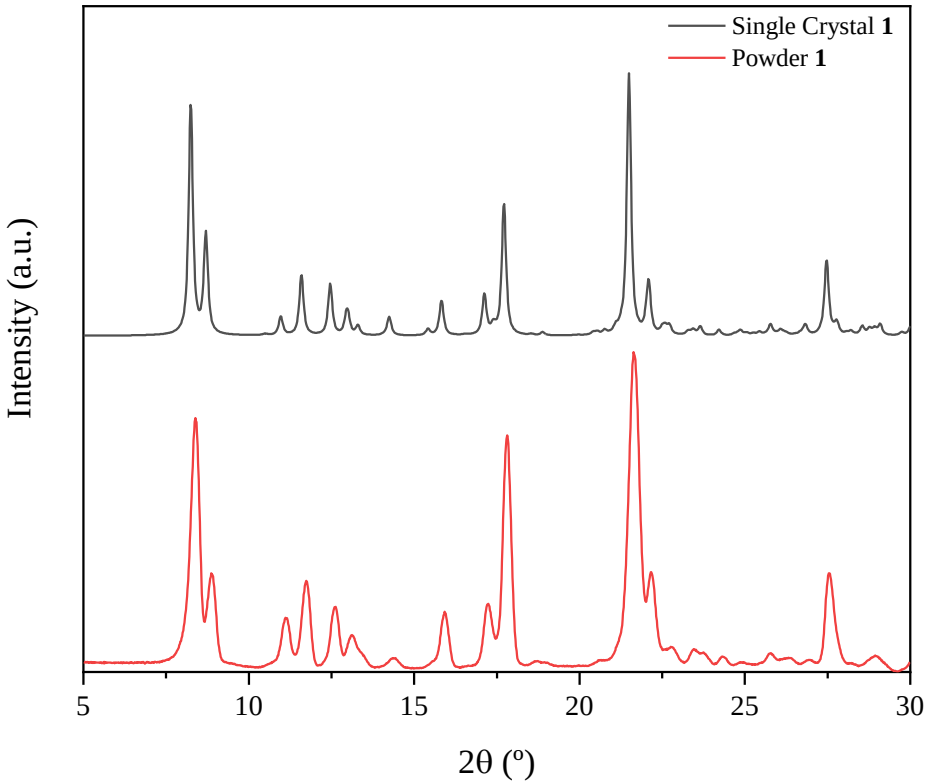

Figure S1. XRD patterns from single crystal collected data at 100 K and powder XRD pattern at 298 K of compound $[Zn(\mu\text{-}2\text{-}FA)(2\text{-}FA)(Isn)_2]_2$ (**1**).

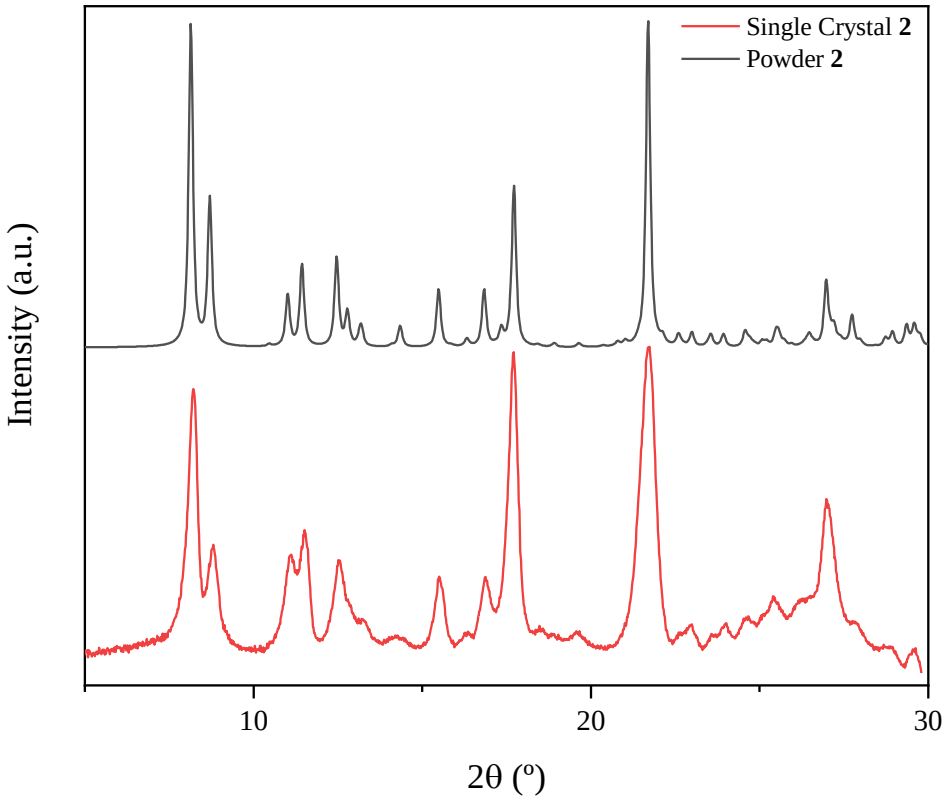

Figure S2. XRD patterns from single crystal collected data at 100 K and powder XRD pattern at 298 K of compound $[Cd(\mu\text{-}2\text{-}FA)(2\text{-}FA)(Isn)_2]_2$ (**2**).

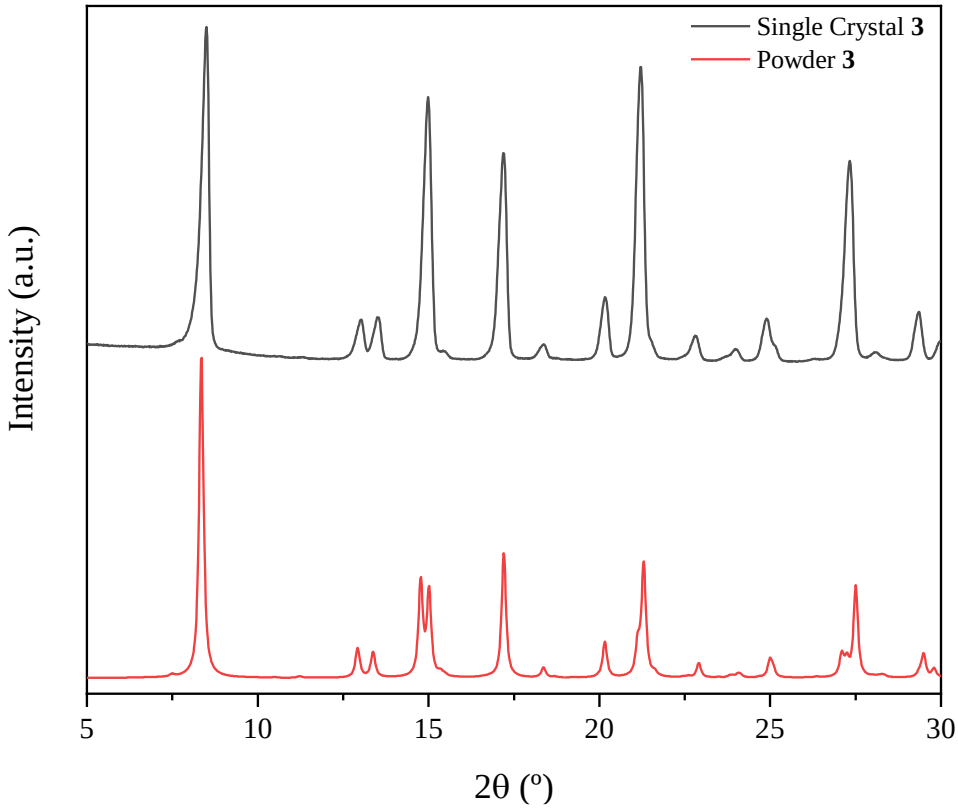

Figure S3. XRD patterns from single crystal collected data at 100 K and powder XRD pattern at 298 K of compound $[Zn(\mu\text{-}2\text{-}FA)_2(4\text{-}Acpy)]_2$ (**3**).

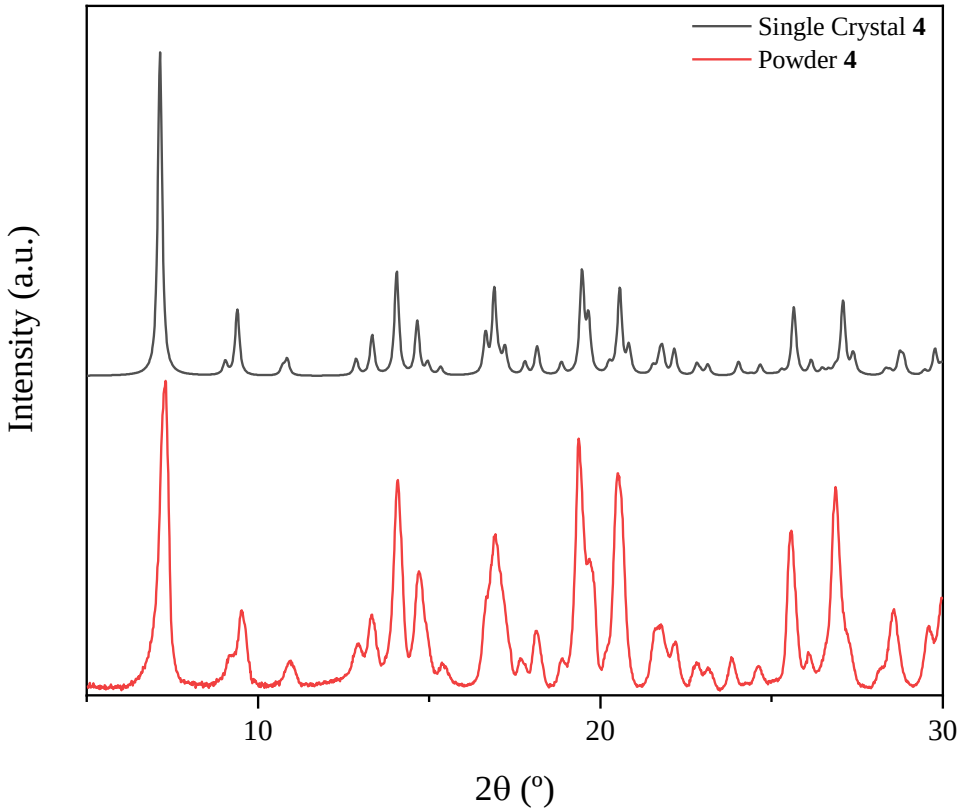

Figure S4. XRD patterns from single crystal collected data at 100 K and powder XRD pattern at 298 K of compound $[Cd(2\text{-}FA)_2(4\text{-}Acpy)_2(OH_2)]$ (**4**).

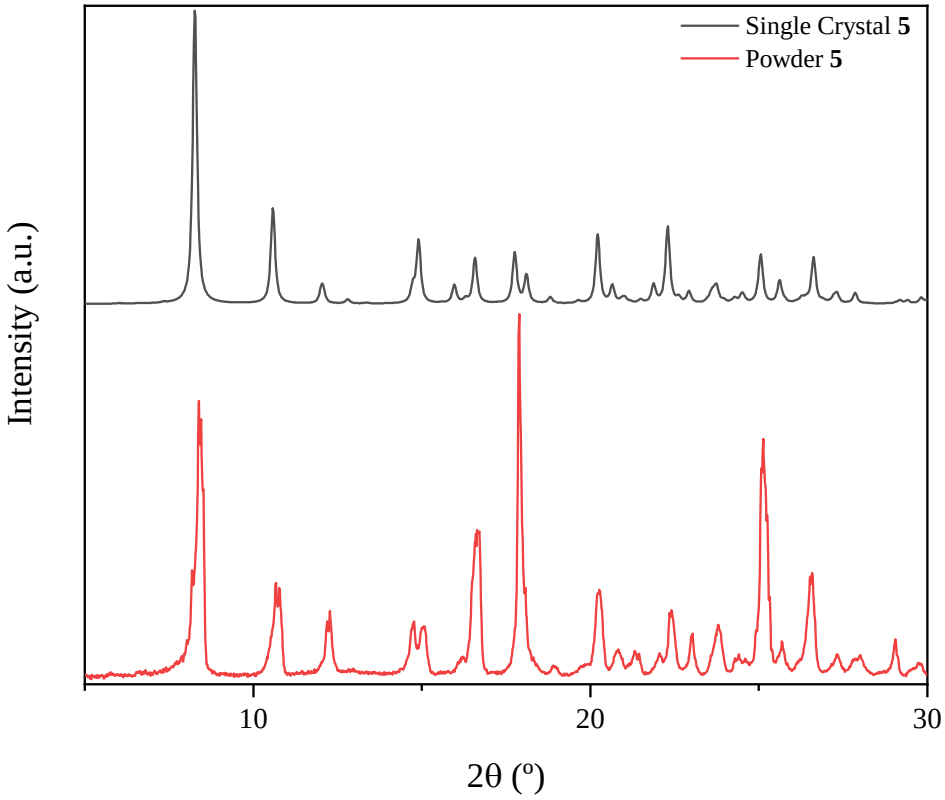

Figure S5. XRD patterns from single crystal collected data at 100 K and powder XRD pattern at 298 K of compound {[Cd(μ-2-FA)$_2$(OH$_2$)$_2$]$_n$[Cd(μ-2-FA)$_2$(4-Acpy)(OH$_2$)]$_n$} (**5**).

Thermogravimetric analysis

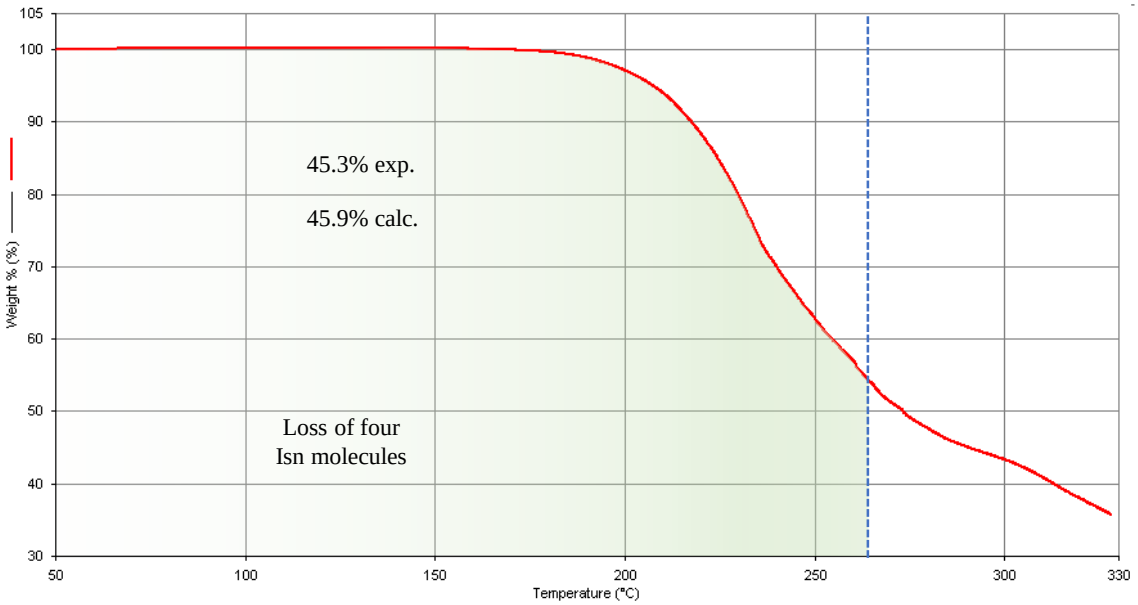

Figure S6. TGA of compound [Zn(μ-2-FA)(2-FA)(Isn)$_2$]$_2$ (**1**) recorded from 50 ºC to 330 ºC.

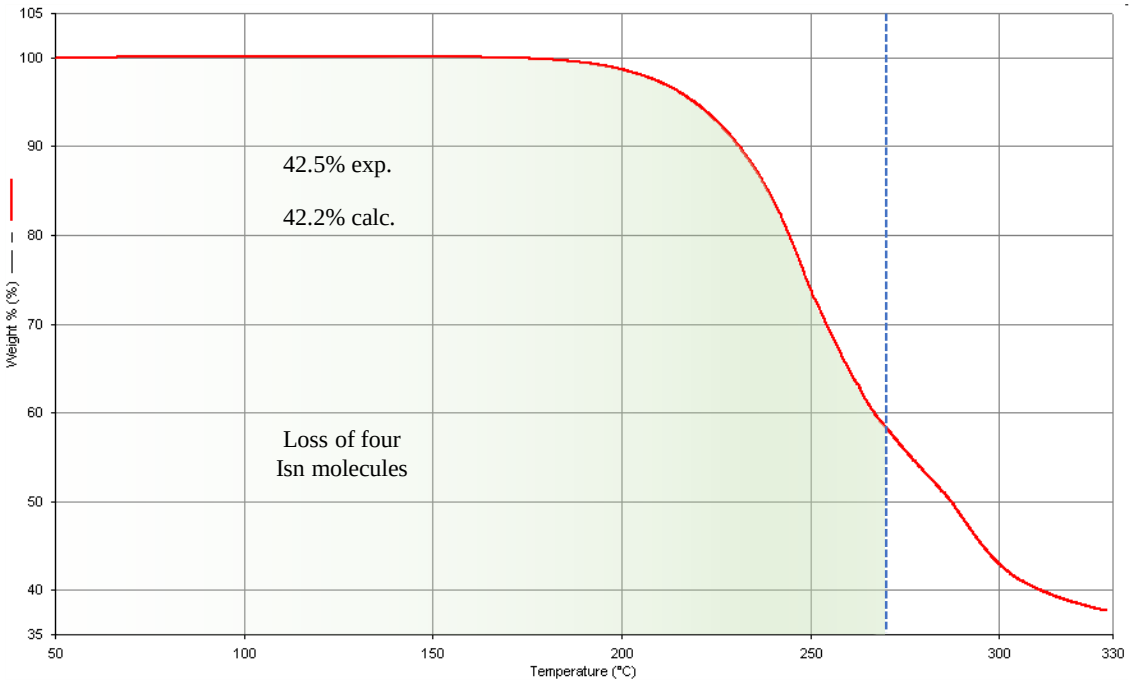

Figure S7. TGA of compound $[Cd(\mu\text{-}2\text{-}FA)(2\text{-}FA)(Isn)_2]_2$ (**2**) recorded from 50 ºC to 330 ºC.

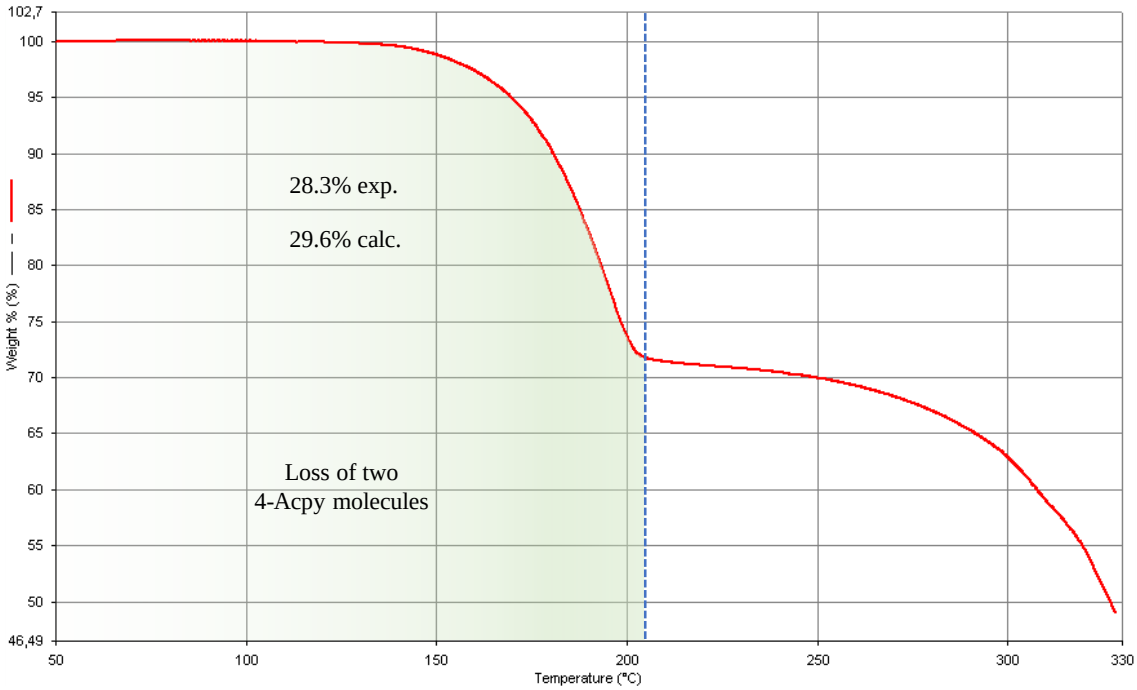

Figure S8. TGA of compound $[Zn(\mu\text{-}2\text{-}FA)_2(4\text{-}Acpy)]_2$ (**3**) recorded from 50 ºC to 330 ºC.

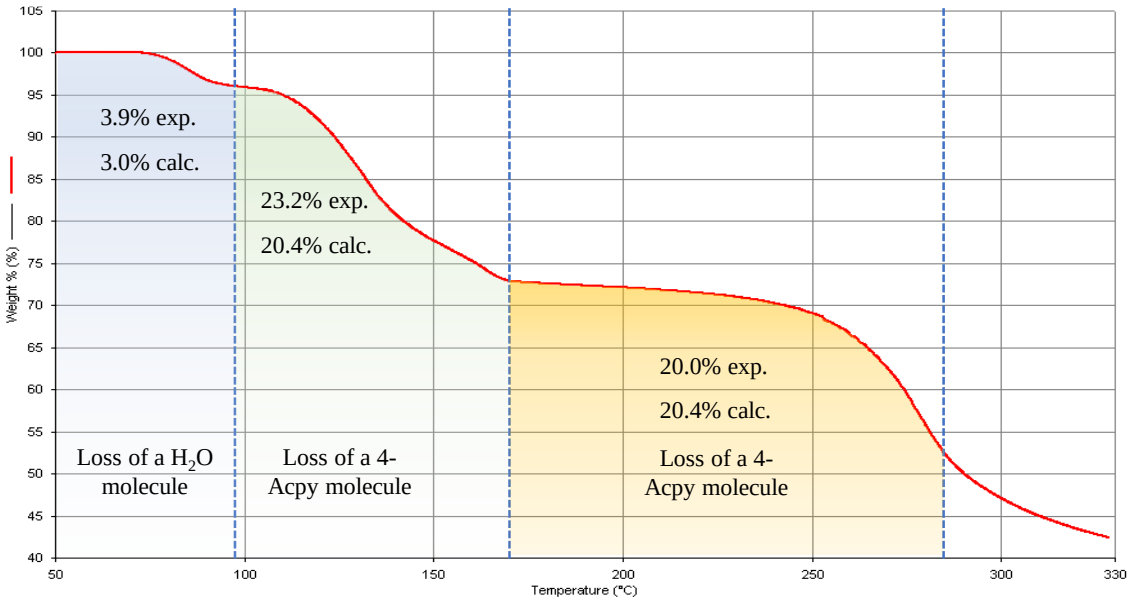

Figure S9. TGA of compound $[Cd(2\text{-}FA)_2(4\text{-}Acpy)_2(OH_2)]$ (**4**) recorded from 50 ºC to 330 ºC.

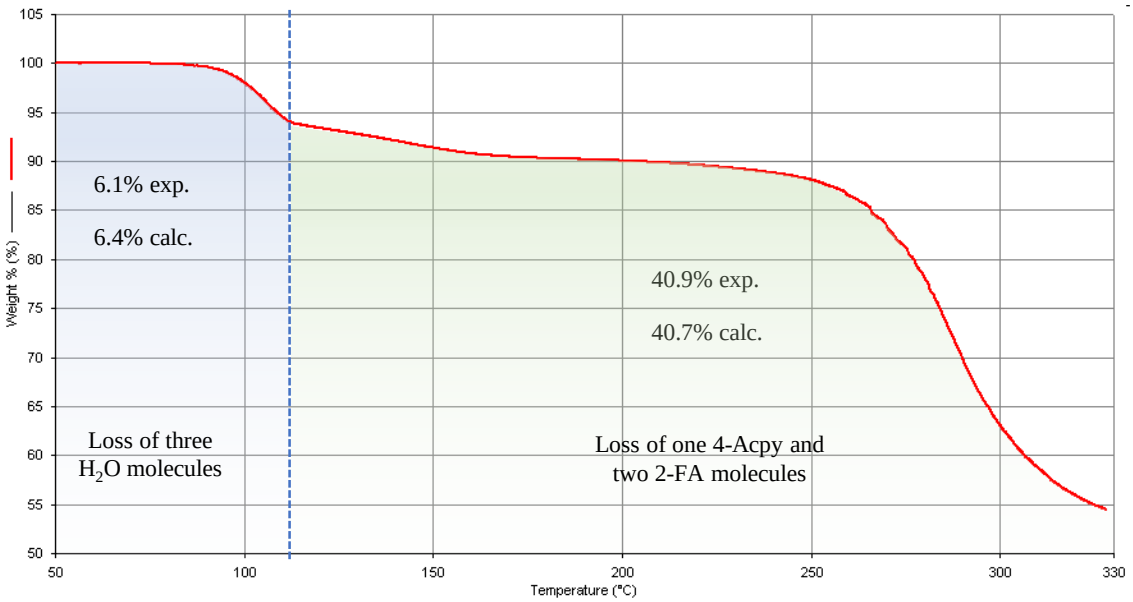

Figure S10. TGA of compound $\{[Cd(\mu\text{-}2\text{-}FA)_2(OH_2)_2]_n[Cd(\mu\text{-}2\text{-}FA)_2(4\text{-}Acpy)(OH_2)]_n\}$ (**5**) recorded from 50 ºC to 330 ºC.

FTIR-ATR, ^{1}H and $^{13}C\{^{1}H\}$ spectroscopies

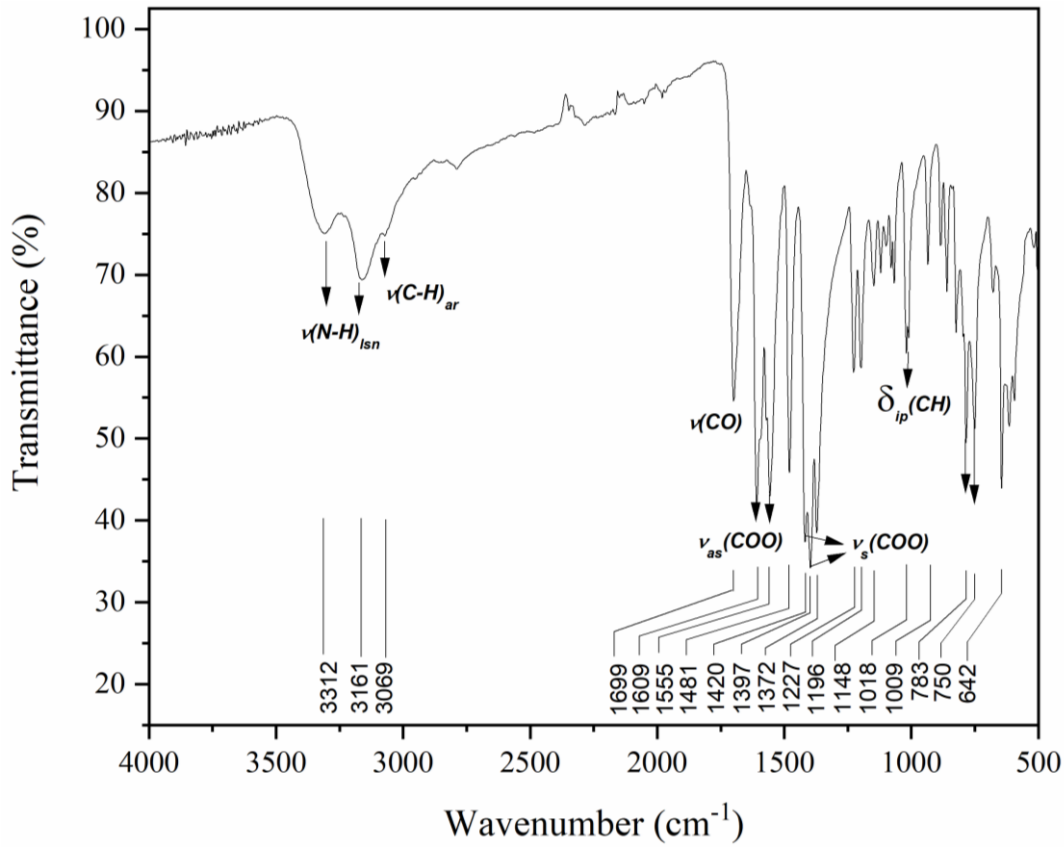

Figure S11. FTIR-ATR spectrum of compound $[Zn(\mu\text{-}2\text{-}FA)(2\text{-}FA)(Isn)_2]_2$ (**1**).

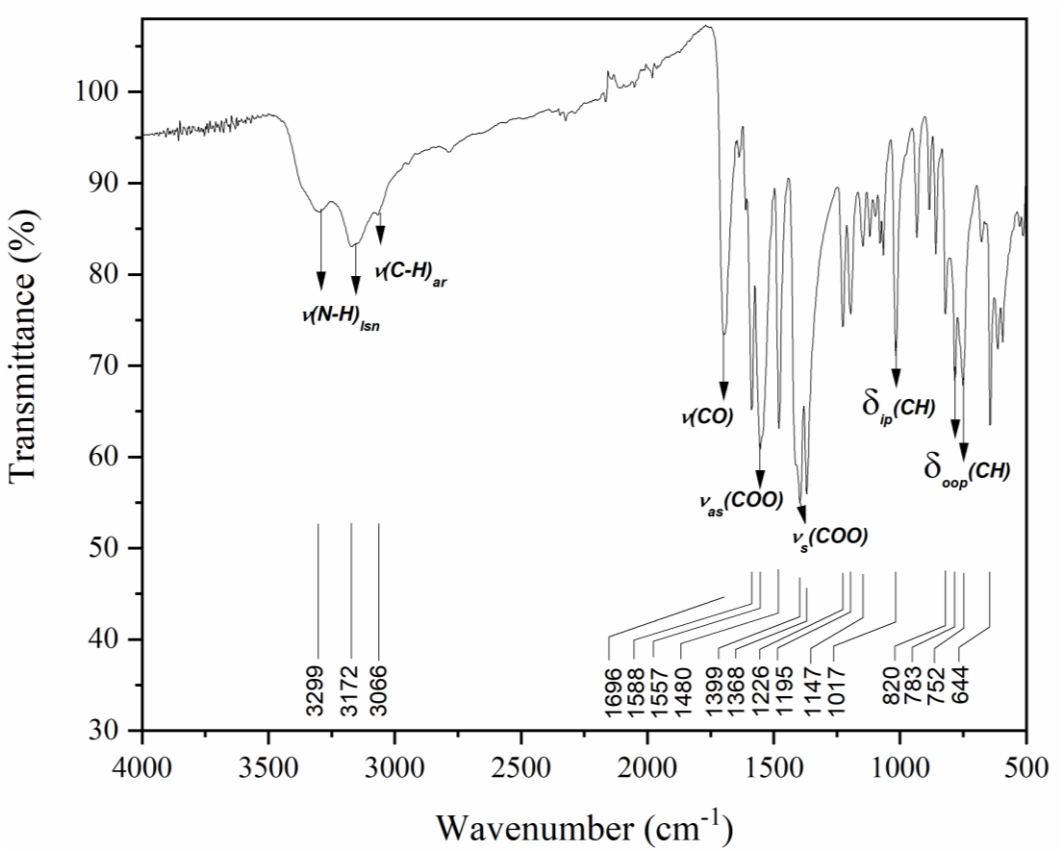

Figure S12. FTIR-ATR spectrum of compound $[Cd(\mu\text{-}2\text{-}FA)(2\text{-}FA)(Isn)_2]_2$ (**2**).

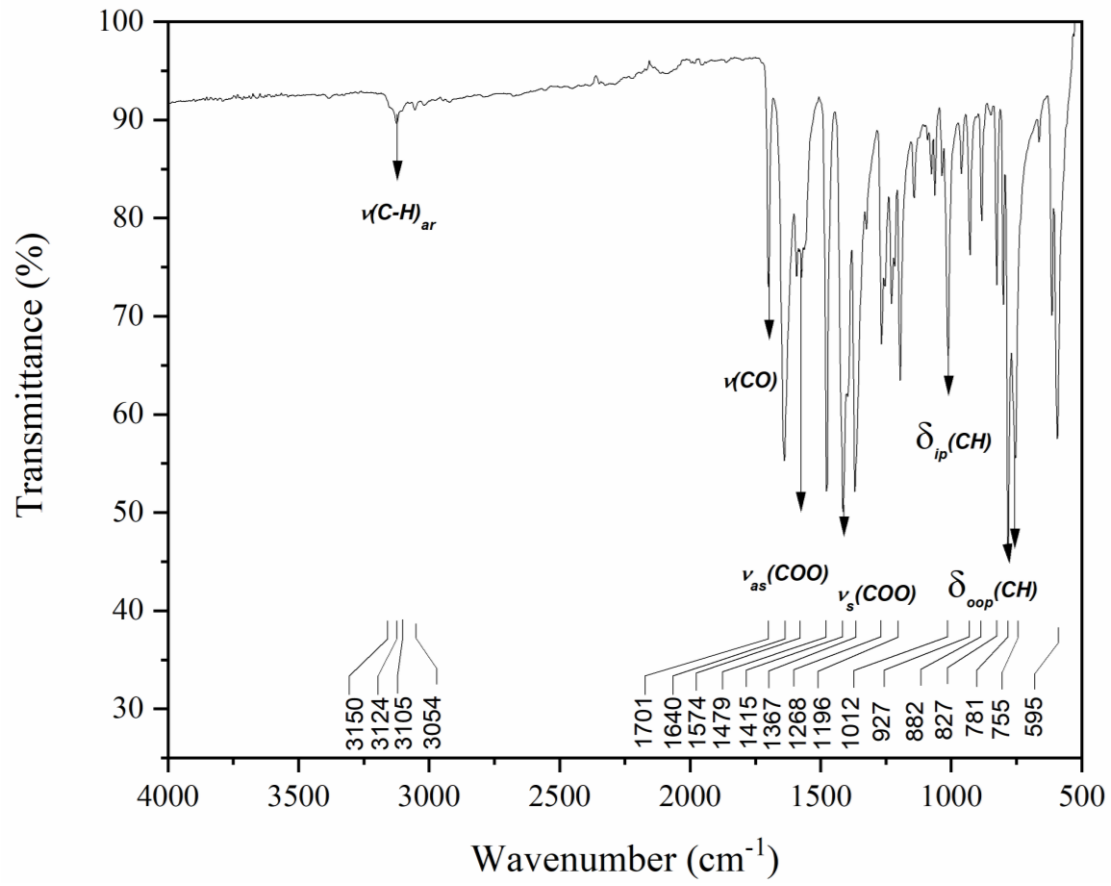

Figure S13. FTIR-ATR spectrum of compound $[Zn(\mu\text{-}2\text{-}FA)_2(4\text{-}Acpy)]_2$ (**3**).

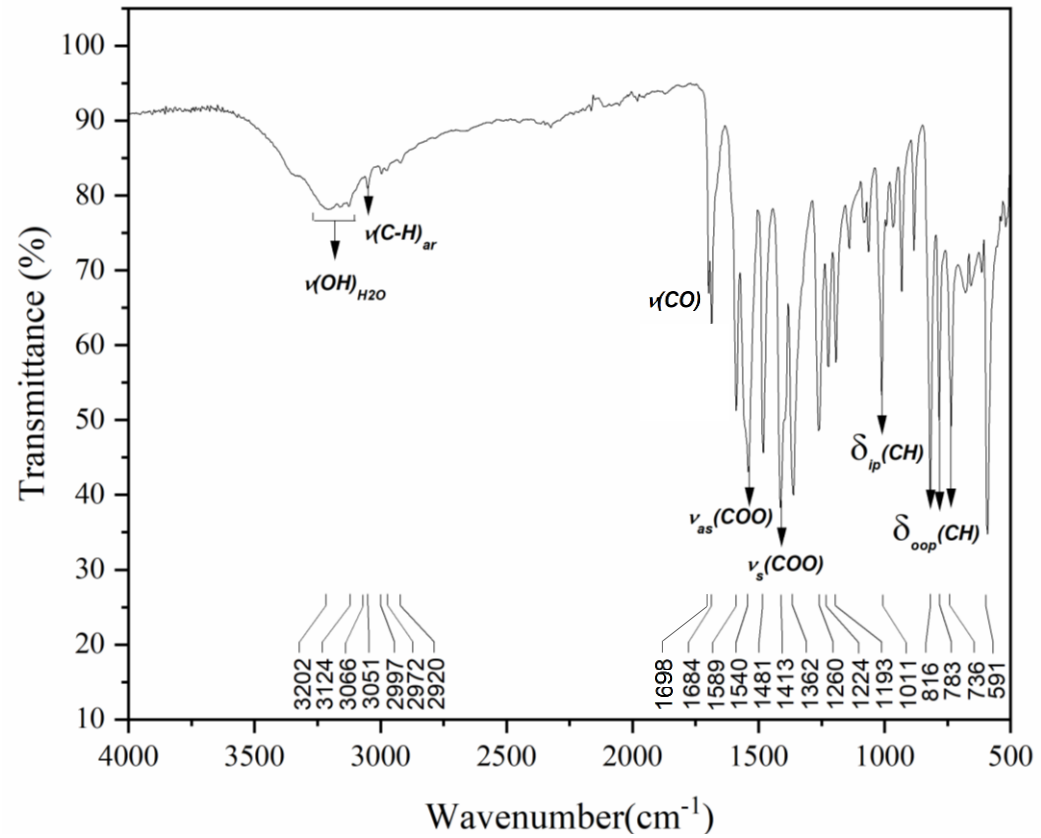

Figure S14. FTIR-ATR spectrum of compound $[Cd(2\text{-}FA)_2(4\text{-}Acpy)_2(OH_2)]$ (**4**).

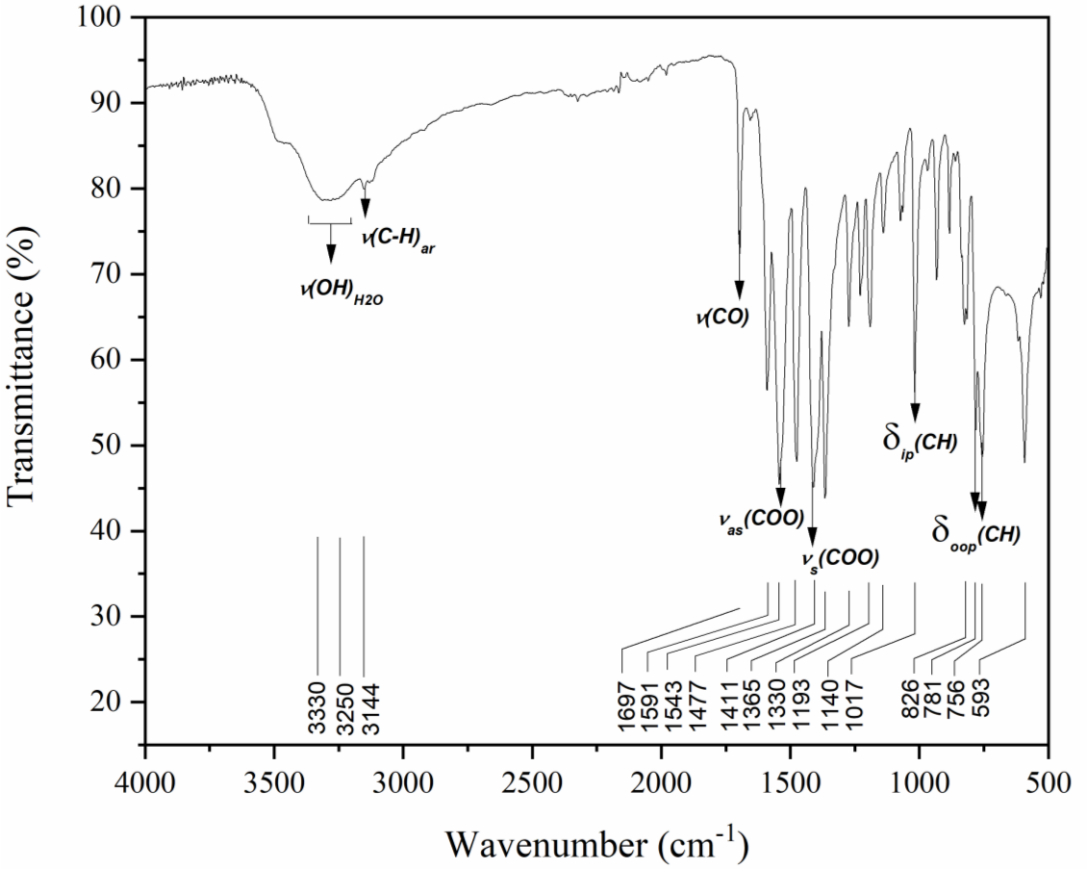

Figure S15. FTIR-ATR spectrum of compound {[Cd(μ-2-FA)$_2$(OH$_2$)$_2$]$_n$[Cd(μ-2-FA)$_2$(4-Acpy)(OH$_2$)]$_n$} (**5**).

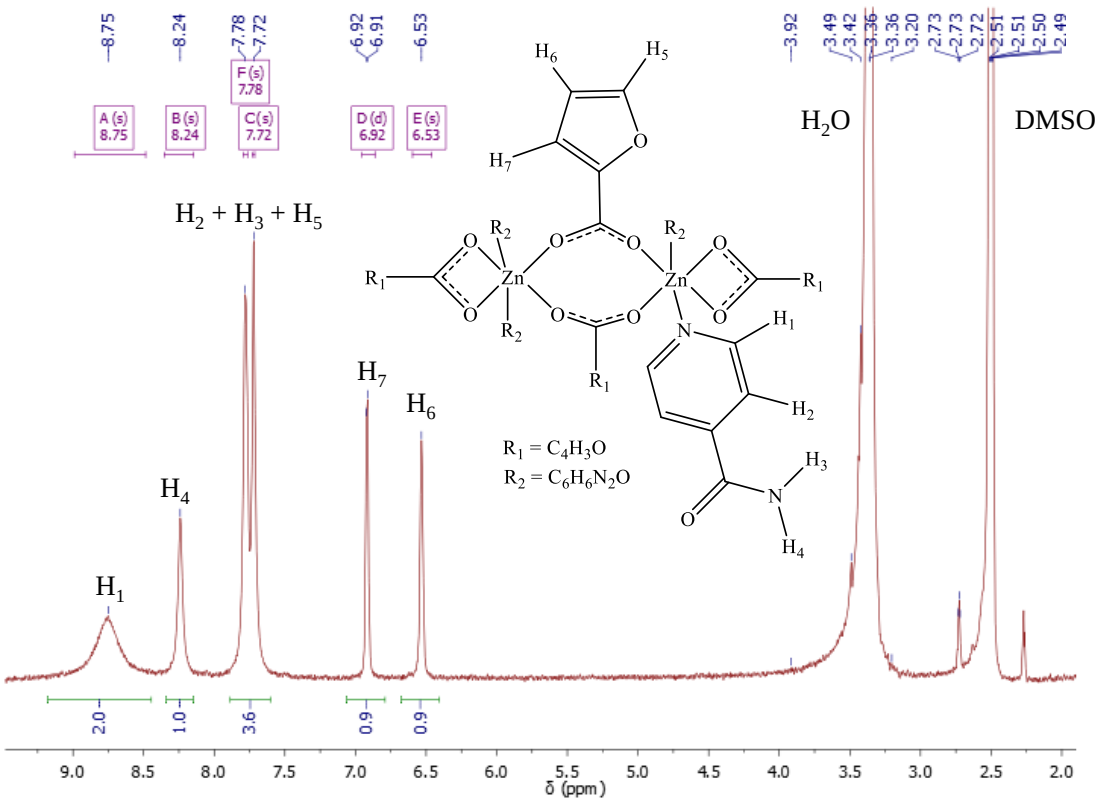

Figure S16. ^{1}H NMR spectrum of compound [Zn(μ-2-FA)(2-FA)(Isn)$_2$]$_2$ (**1**).

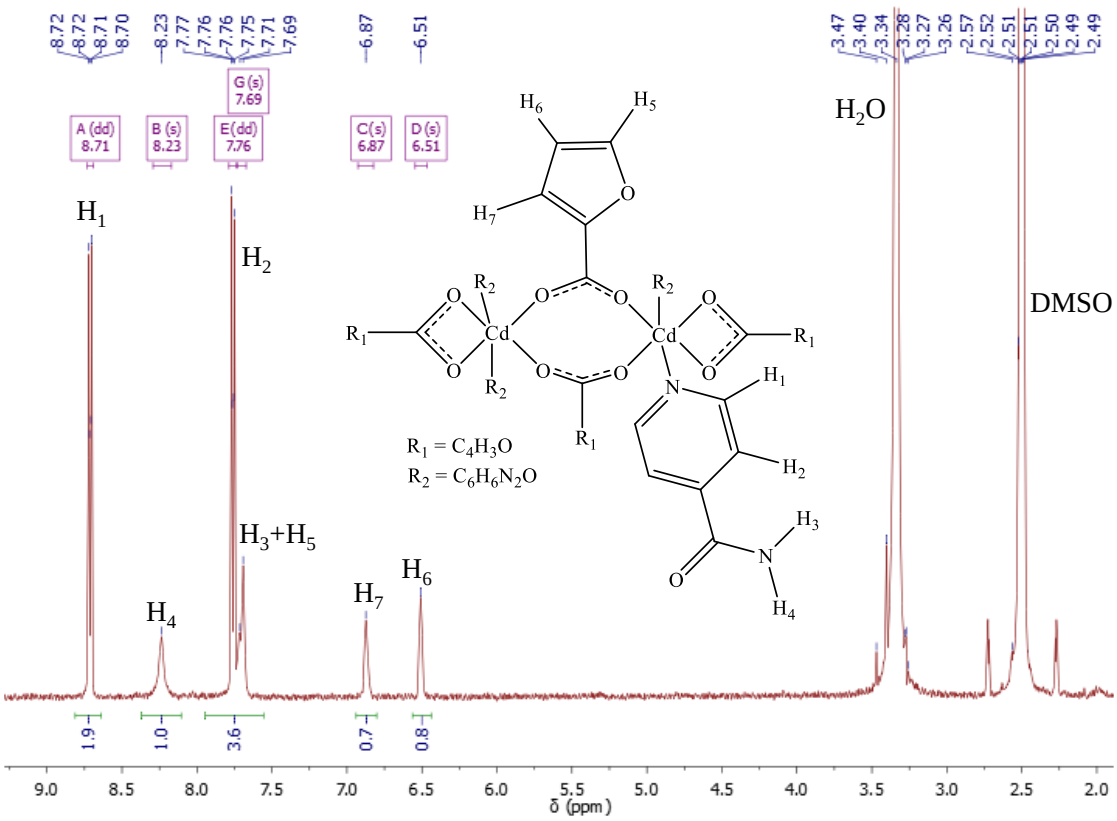

Figure S17. ^{1}H NMR spectrum of compound [Cd(μ-2-FA)(2-FA)(Isn)$_2$]$_2$ (**2**).

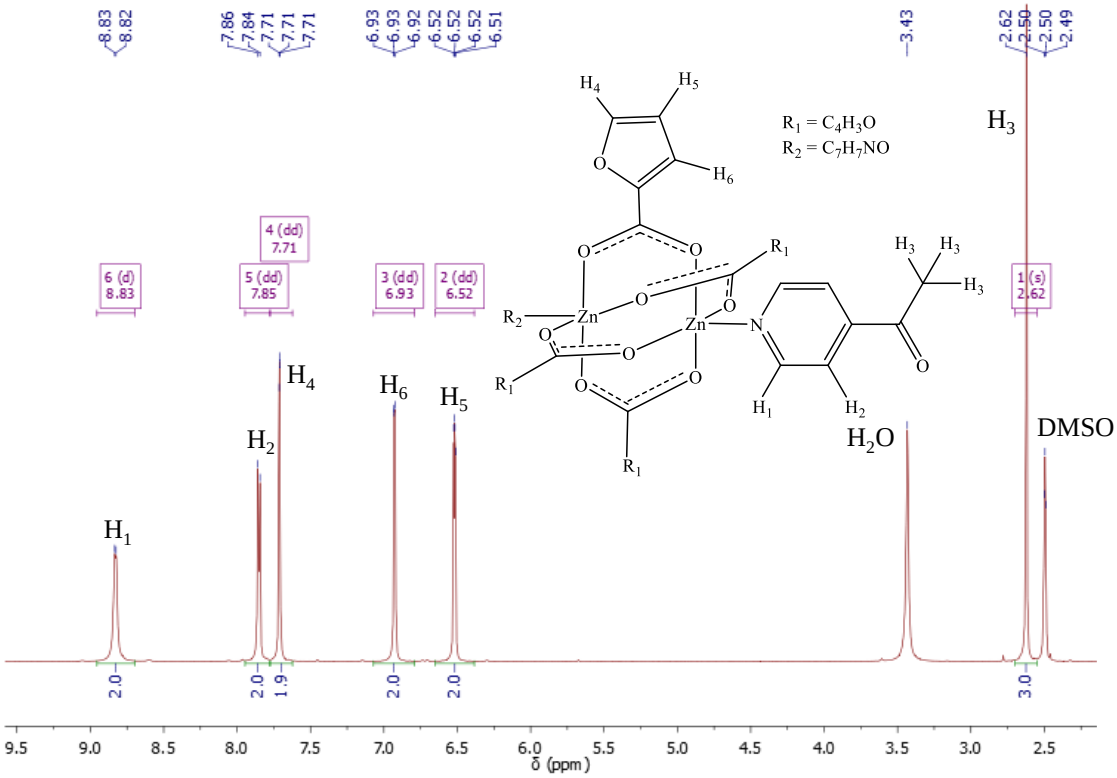

Figure S18. ^{1}H NMR spectrum of compound [Zn(μ-2-FA)$_2$(4-Acpy)]$_2$ (**3**).

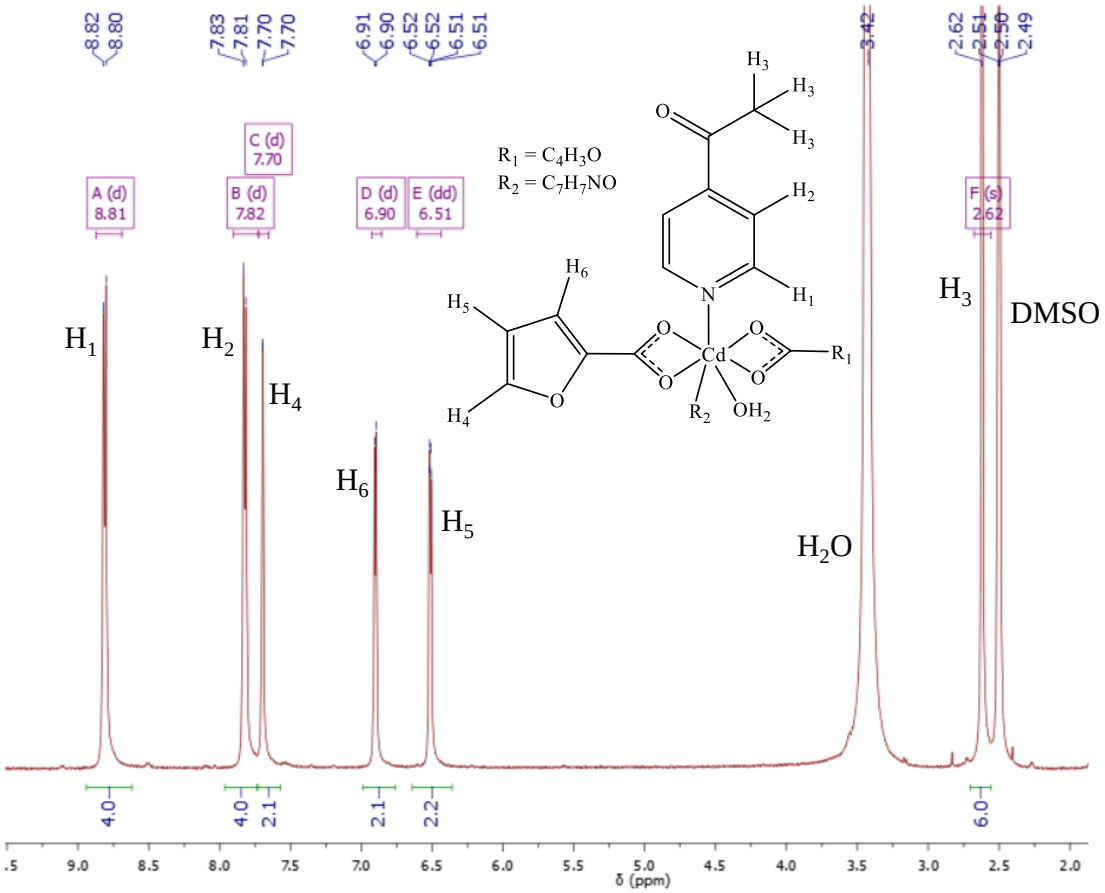

Figure S19. ^{1}H NMR spectrum of compound [Cd(2-FA)$_2$(4-Acpy)$_2$(OH$_2$)] (**4**).

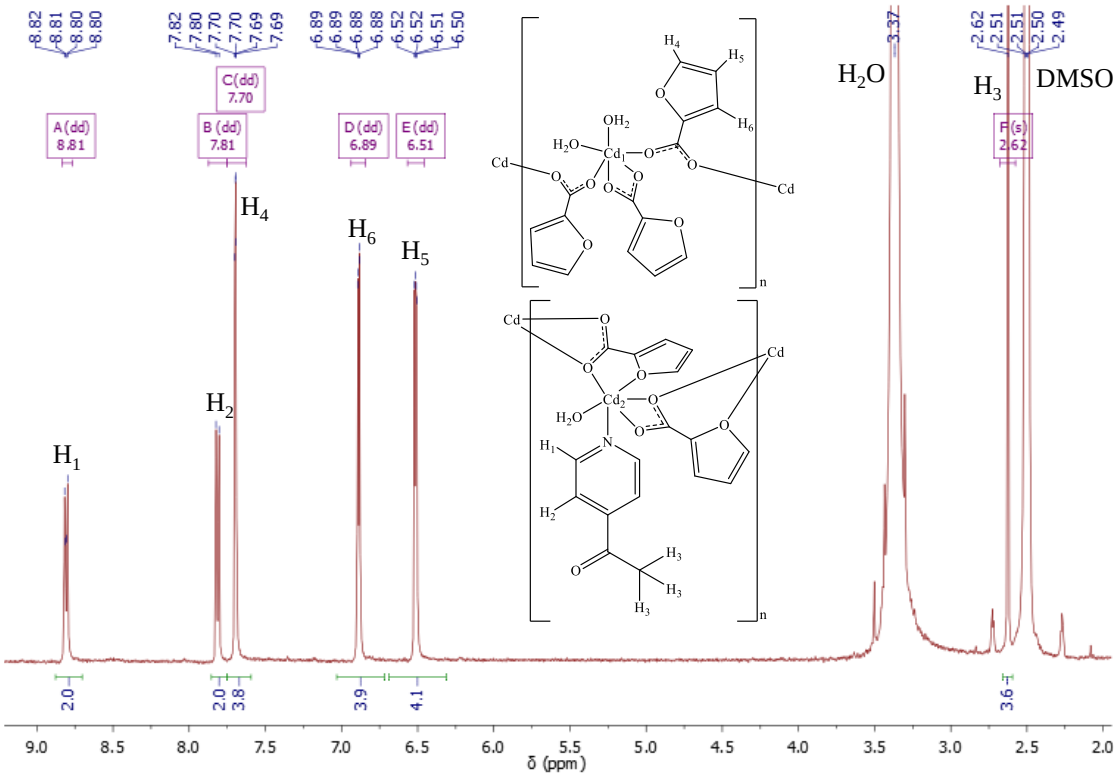

Figure S20. ^{1}H NMR spectrum of compound {[Cd(μ-2-FA)$_2$(OH$_2$)$_2$]$_n$[Cd(μ-2-FA)$_2$(4-Acpy)(OH$_2$)]$_n$} (**5**).

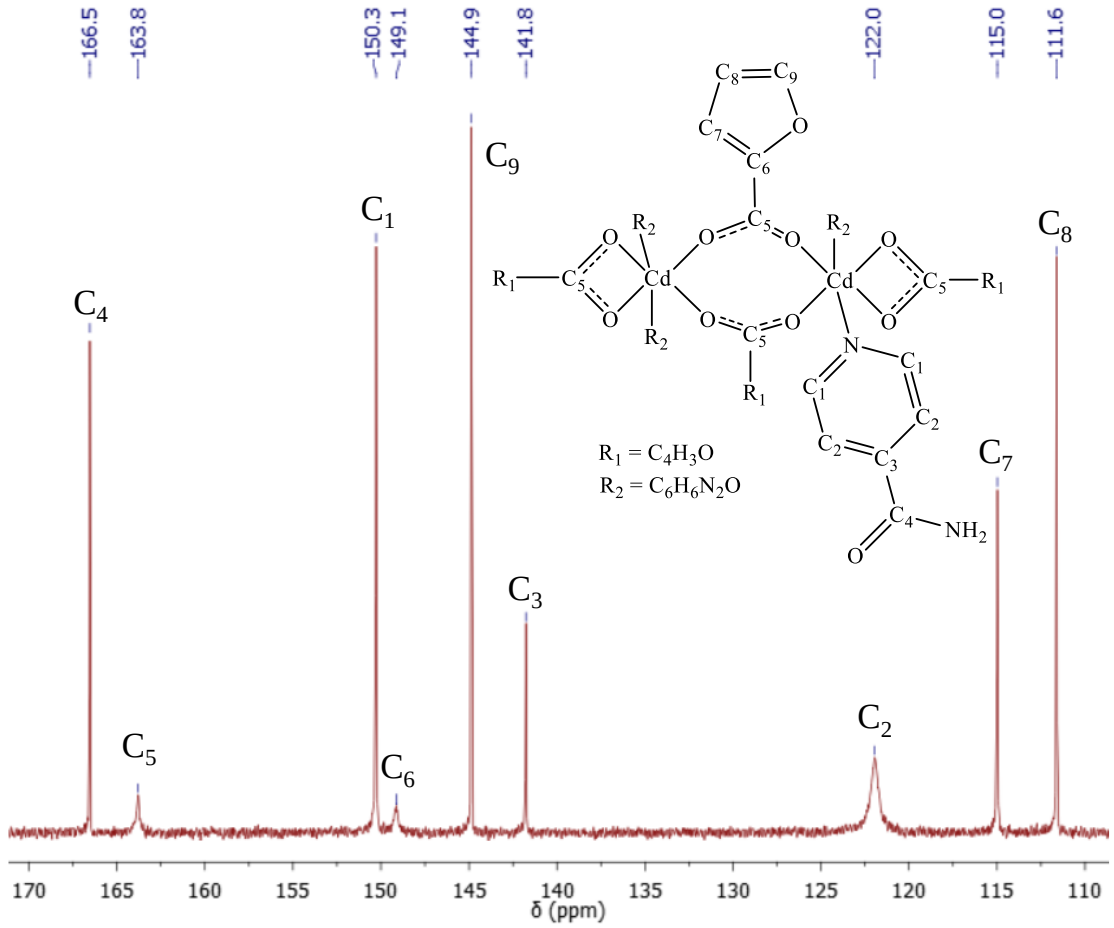

Figure S21. $^{13}C\{^{1}H\}$ NMR spectra of compound $[Zn(\mu\text{-}2\text{-}FA)(2\text{-}FA)(Isn)_2]_2$ (**1**).

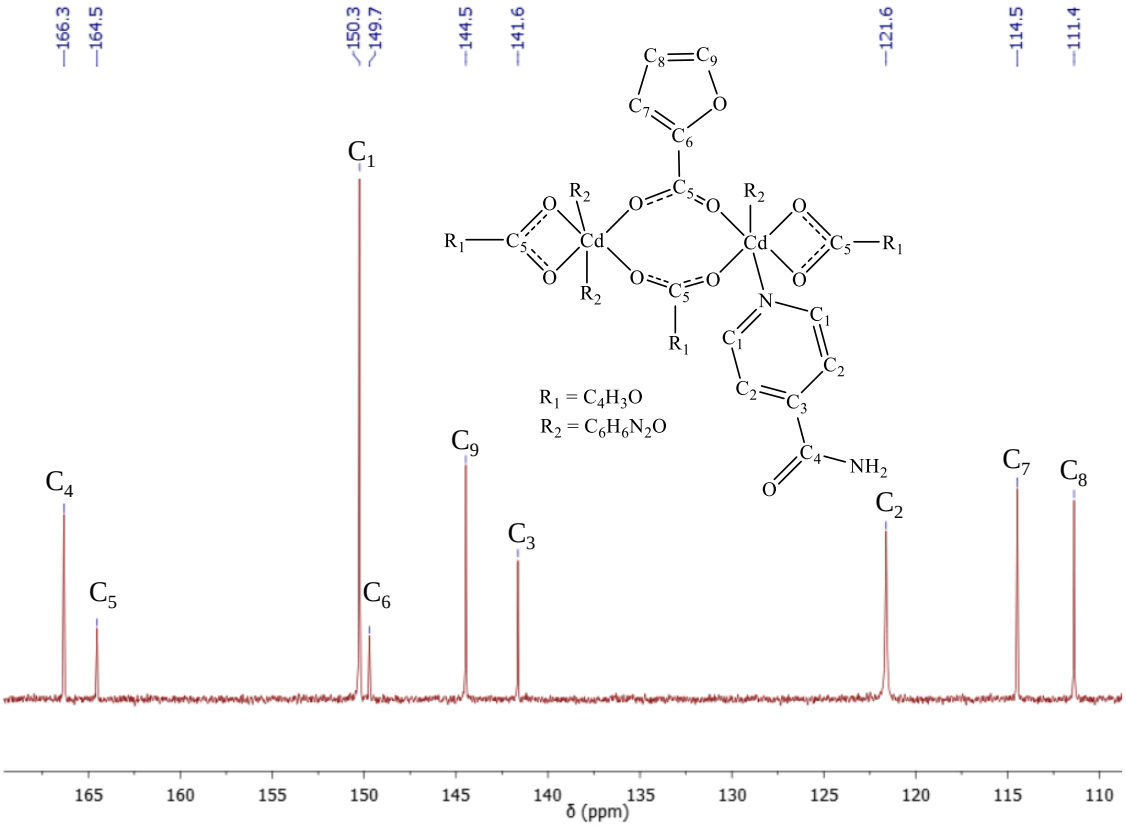

Figure S22. $^{13}C\{^{1}H\}$ NMR spectra of compound $[Cd(\mu\text{-}2\text{-}FA)(2\text{-}FA)(Isn)_2]_2$ (**2**).

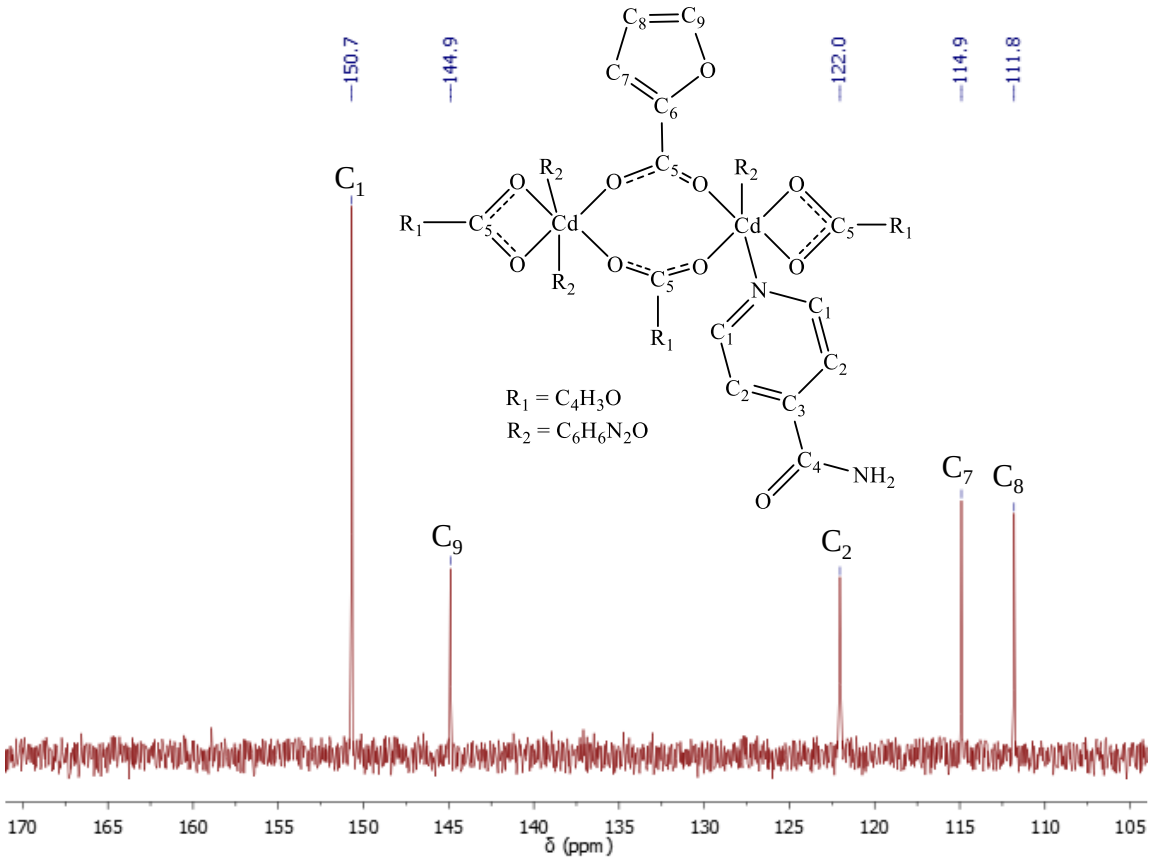

Figure S23. DEPT-135 NMR spectra of compound $[Cd(\mu\text{-}2\text{-}FA)(2\text{-}FA)(Isn)_2]_2$ (**2**).

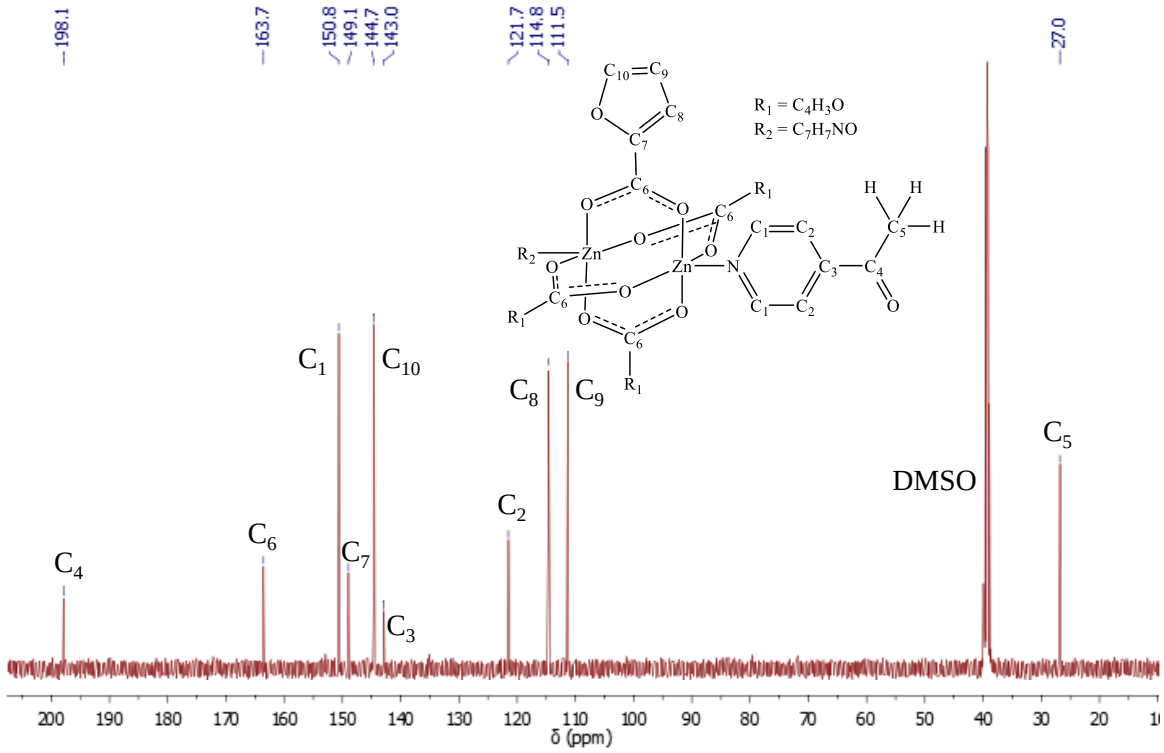

Figure S24. $^{13}C\{^1H\}$ NMR spectra of compound $[Zn(\mu\text{-}2\text{-}FA)_2(4\text{-}Acpy)]_2$ (**3**).

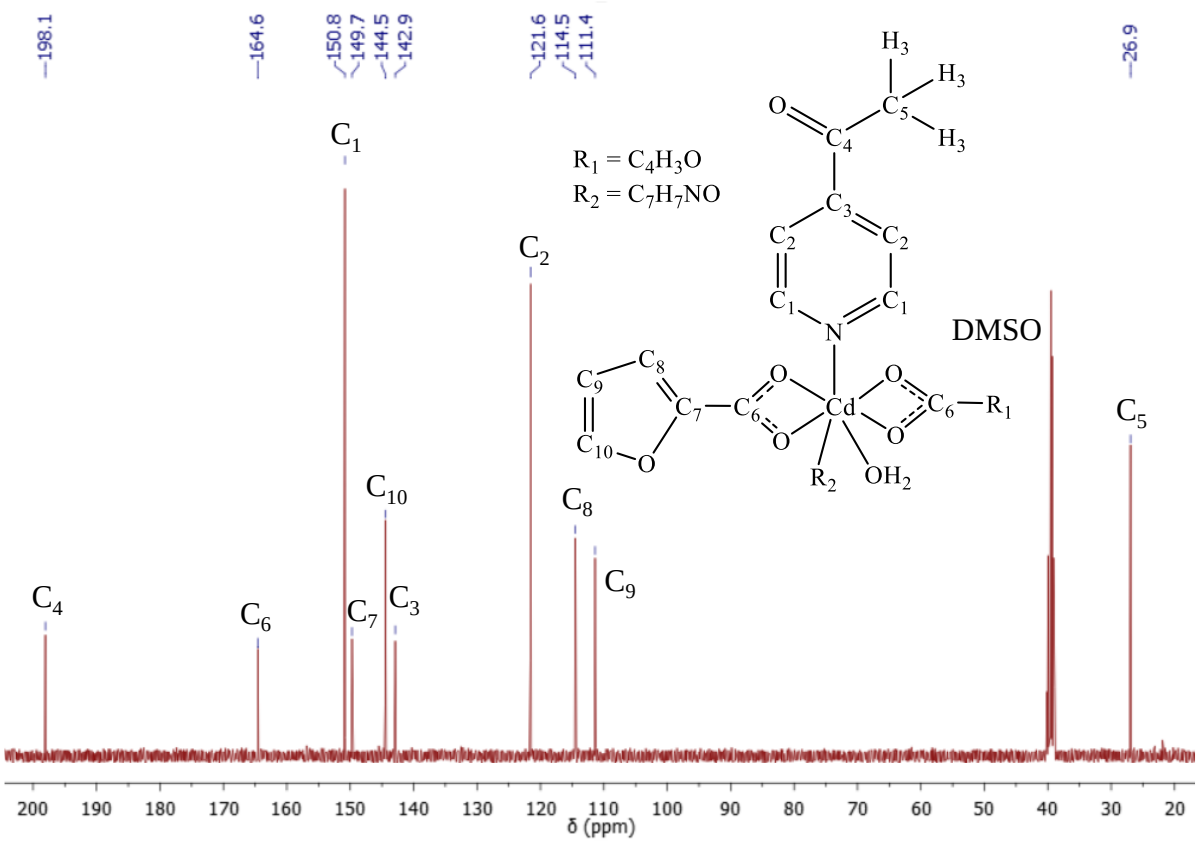

Figure S25. $^{13}C\{^{1}H\}$ NMR spectra of compound $[Cd(2\text{-}FA)_2(4\text{-}Acpy)_2(OH_2)]$ (**4**).

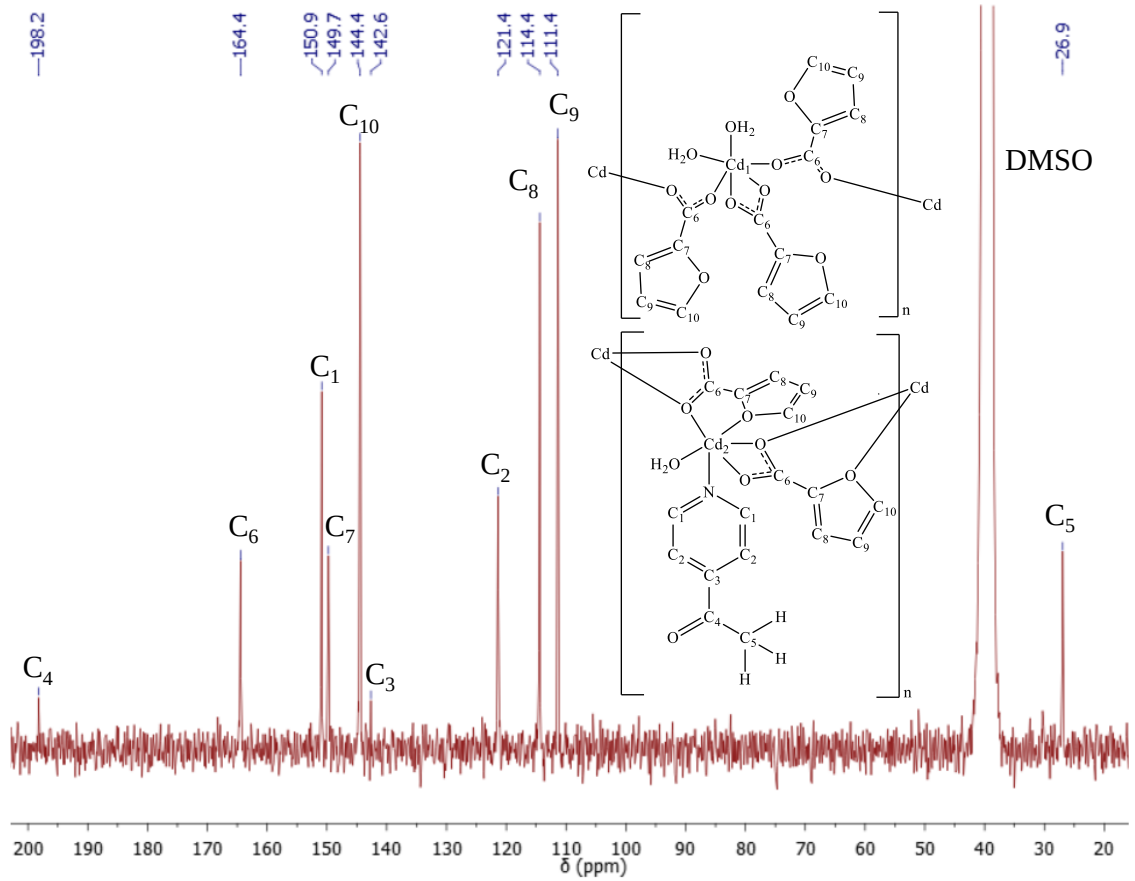

Figure S26. $^{13}C\{^{1}H\}$ NMR spectra of compound $[Cd(2\text{-}FA)_2(OH_2)_2]_n[Cd(2\text{-}FA)_2(4\text{-}Acpy)(OH_2)]_n$ (**5**).

Geometric Evaluation

Table S1. Geometry distortion analysis of the Zn(II) and Cd(II) *cores* from **1-5** using *S* parameter calculated with SHAPE.[1,2]

Compound	Label	Geometry[a]	*S* value
1	Zn(1)	**OC-6**	**6.229**
		TPR-6	8.205
2	Cd(1)	**OC-6**	**3.807**
		TPR-6	11.205
3	Zn(1)	vOC-5	0.969
		TBPY-5	5.417
		SPY-5	**0.199**
		JTBPY-5	8.068
	Zn(2)	vOC-5	0.887
		TBPY-5	5.432
		SPY-5	**0.175**
		JTBPY-5	7.980
4	Cd(1)	**PBPY-7**	**2.773**
		COC-7	6.222
		CTPR-7	4.805
		JPBPY-7	6.107
5	Cd(1)	CU-8	14.862
		SAPR-8	6.675
		TDD-8	4.316
		JGBF-8	13.844
		JBTP-8	3.364
		BTPR-8	4.158
		JSD-8	4.018
		TT-8	14.518
		PBPY-7	8.756
		COC-7	4.611
		CTPR-7	3.262
		JPBPY-7	9.815
		PPY-6	11.044
		TPR-6	**2.895**
	Cd(2)	**PBPY-7**	**1.213**
		COC-7	8.100
		CTPR-7	6.607
		JPBPY-7	3.849

Closer values have been highlighted in bold. vOC-5 = Vacant octahedron; TBPY-5 = Trigonal bipyramid; SPY-5 = Square pyramid; JTBPY-5 = Johnson trigonal bipyramid; PPY-6 = Pentagonal pyramid; OC-6 = Octahedron; TPR-6 = Trigonal prism; PBPY-7 = Pentagonal bipyramid; COC-7 = Capped octahedron; CTPR-7 = Capped trigonal prism; JPBPY-7 = Johnson pentagonal bipyramid; CU-8 = Cube; SAPR-8 = Square antiprism; TDD-8 = Triangular dodecahedron; JGBF-8 = Johnson - Gyrobifastigium; JBTP-8 = Johnson – Biaugmented trigonal prism; BTPR-8 = Biaugmented trigonal prism; JSD-8 = Snub disphenoid; TT-8 = Triakis tetrahedron.

Extended structures

Compounds **1** and **2**. The intermolecular interactions of **1** and **2** are mainly directed by amide-amide homosynthons between the Isn ligands, which associate dimeric units along the [101] direction. In addition, the H-bond interactions involving the *anti H*-atom of the Isn ligands and the oxygen atom from the μ_2-η^2-2-FA, as well as other additional C-H··O interactions form the final 3D networks (Fig. S17). Relevant distances have been listed in Table S2.

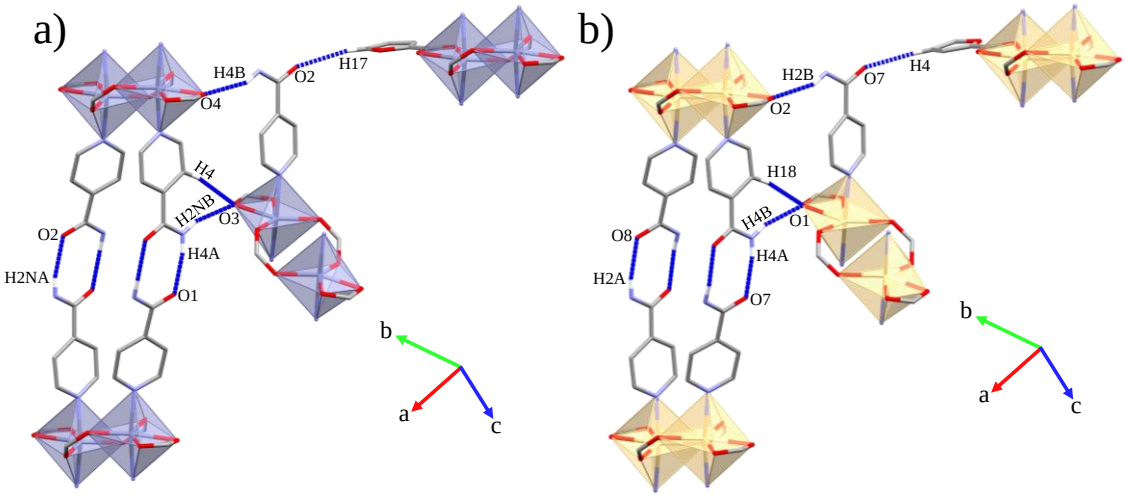

Figure S27. Supramolecular expansion of (a) **1** and (b) **2**. Hydrogen atoms not involved in the intermolecular interactions have been omitted for clarity.

Table S2. Intermolecular interactions present in complexes **1** and **2**.

1	D-H···A	D-H (Å)	H···A (Å)	D···A (Å)	>D-H···A (°)
	N(2)-H(2NA)···O(2)	0.88	2.06	2.930(4)	168
	N(4)-H(4A)···O(1)	0.88	2.00	2.877(4)	175
	N(2)-H(2NB)···O(3)	0.88	2.06	2.904(4)	159
	N(4)-H(4B)···O(4)	0.88	2.08	2.891(5)	153
	C(4)-H(4)···O(3)	0.95	2.32	3.252(6)	165
	C(17)-H(17)···O(2)	0.95	2.43	3.359(7)	165
2	D-H···A	D-H (Å)	H···A (Å)	D···A (Å)	>D-H···A (°)
	N(2)-H(2A)···O(8)	0.88	2.00	2.867(5)	169
	N(4)-H(4A)···O(7)	0.88	2.06	2.933(5)	170
	N(2)-H(2NB)···O(2)	0.88	2.07	2.900(6)	156
	N(4)-H(4B)···O(1)	0.88	2.08	2.928(6)	162
	C(4)-H(4)···O(7)	0.95	2.33	3.246(8)	162
	C(18)-H(18)···O(1)	0.95	2.25	3.188(6)	168

Compound **3**. The supramolecular expansion of **3** is supported by two groups of three-stacked rings by π···π interactions along both [1$\bar{1}$0] and [110] in a 2-FA, 4-Acpy, and 2-FA sequence (Fig. S18a) resulting in the assembly of a 3D supramolecular net. Besides, these π···π interactions are supported by C-H···O associations between $O_{4\text{-Acpy}}$

and *H* atoms from 2-FA units and between methyl and *O* atom from the furane ring (Fig. 18b). Relevant distances have been listed in Table S3.

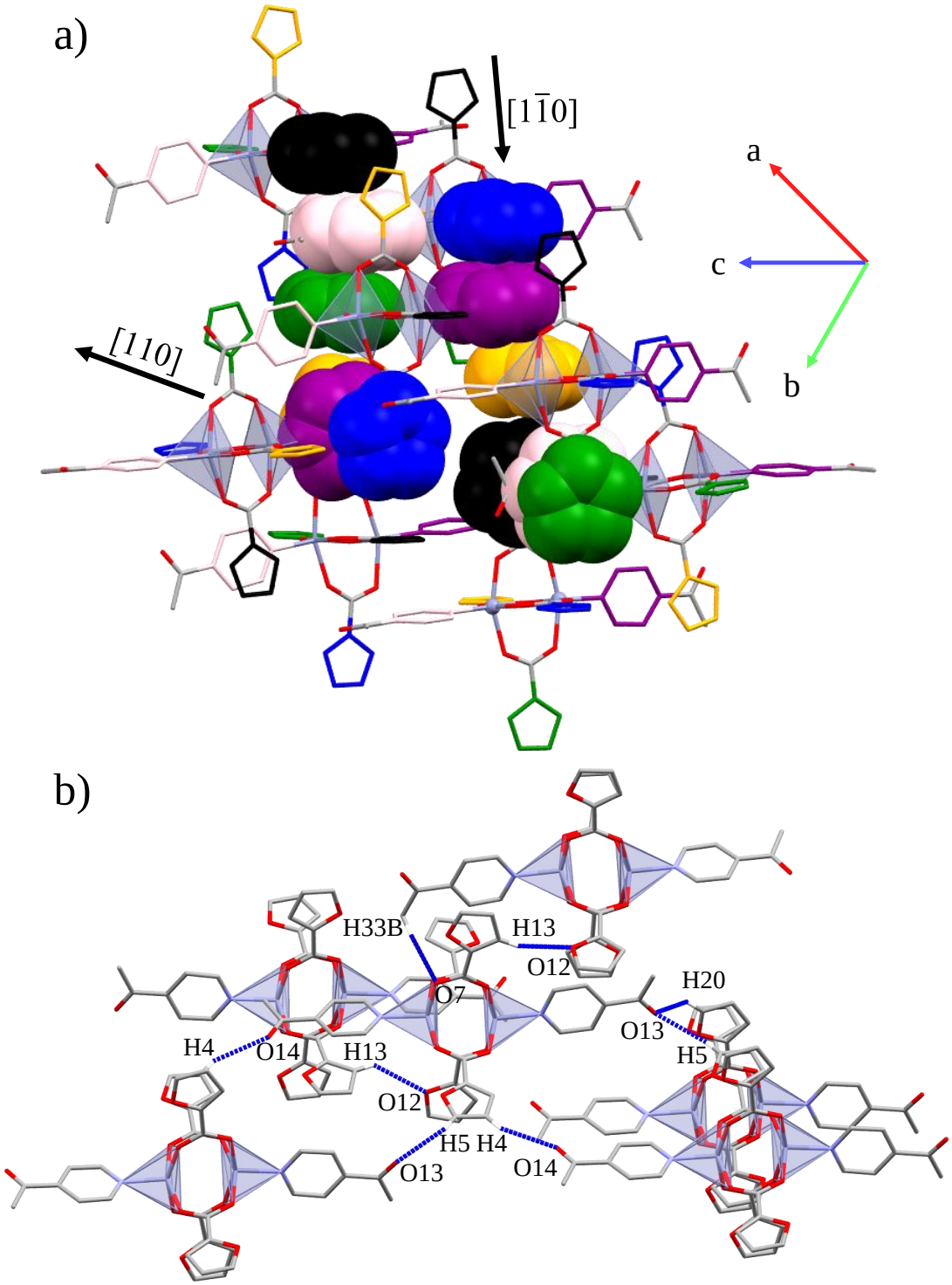

Figure S28. Supramolecular expansion of **3** supported by (a) π···π and (b) C-H···O interactions. Hydrogen atoms not involved in the intermolecular interactions have been omitted for clarity.

Table S3. Intermolecular interactions present in **3**.

D-H···A		D-H (Å)		H···A (Å)	D···A (Å)	>D-H···A (º)
C(4)-H(4)···O(14)		0.930		2.642	3.366(5)	135.1
C(5)-H(5)···O(13)		0.930		2.585	3.391(5)	145.2
C(13)-H(13)···O(12)		0.930		2.607	3.317(5)	133.6
C(20)-H(20)···O(13)		0.930		2.488	3.243(5)	138.4
C(33)-H(33B)···O(7)		0.959		2.571	3.521(5)	170.5
π···π interactions						
Cg(I)···Cg(J)	Cg···Cg[a] (Å)	α[b] (º)	β, γ[c] (º)		$d_{plane-plane}$[d] (Å)	d_{offset}[e] (Å)
Cg(1)···Cg(5)	3.537(2)	6.79(19)	16.0, 20.5		3.3121(14), 3.3993(16)	0.976
Cg(2)···Cg(5)	3.546(2)	6.94(19)	19.9, 13.2		3.4524(14), 3.3352(15)	1.204
Cg(3)···Cg(6)	3.453(2)	7.09(19)	15.1, 8.5		3.4153(14), 3.3339(15)	0.900
Cg(4)···Cg(6)	3.677(2)	7.95(19)	20.7, 27.1		3.2733(14), 3.4402(15)	1.298

[a]Cg···Cg = distance between ring centroids; [b]α= dihedral angle between Planes I and J; [c]Offset angles: β = angle Cg(I)-Cg(J) and normal to plane I and γ = angle Cg(I)-Cg(J) and normal to plane J (β = γ, when α = 0º); [d]Perpendicular distance of Cg(I) on plane J and perpendicular distance of Cg(J) on plane I (equal when α = 0º); [e]Slippage = Horizontal displacement or slippage between Cg(I) and Cg(J) (equal for both centroids when α = 0º). Cg(1) = O(3) C(2) C(3) C(4) C(5); Cg(2) = O(6) C(7) C(8) C(9) C(10); Cg(3) = O(9) C(12) C(13) C(14) C(15); Cg(4) = O(12) C(17) C(18) C(19) C(20); Cg(5) = N(1) C(21) C(22) C(23) C(24) C(25); Cg(6) = N(2) C(28) C(29) C(30) C(31) C32.

Compound **4**. The supramolecular expansion of **4** is driven by the H-bonds between the water molecules and the carboxylate oxygen atoms, which lengthen the Cd-O bonds (O(2) and O(5)), which form 1D chains along the [100] direction. These chains are supported by weak C-H···O associations between the carbonyl oxygen atoms from 4-Acpy and the methyl hydrogen atoms from nearby 4-Acpy. In addition, there are two types of furoate five-membered rings that display π···π interactions between them extending the supramolecular structure along the [001] direction, conjointly with weak C-H···π interactions involving the methyl H-atoms from 4-Acpy and the five-membered rings from 2-FA. Additional C-H···O interactions between the acetyl groups of 4-Acpy and the carboxylate and H-atoms from 2-FA support the propagation of the structure. The combination of all these interactions extends the structure along the (101) plane forming 2D layers (Fig. S19). Relevant distances have been listed in Table S4.

Table S4. Intermolecular interactions present in **4**.

D-H···A	D-H (Å)	H···A (Å)	D···A	>D-H···A (º)
O(9)-H(9OA)···O(2)	0.80(3)	1.95(4)	2.737(4)	169(3)
O(9)-H(9OB)···O(5)	0.80(4)	1.95(4)	2.731(4)	166(4)
C(8)-H(8)···O(8)	0.95	2.55	3.451(5)	157
C(17)-H(17A)···O(8)	0.98	2.58	3.542(6)	165
C(24)-H(24A)···O(7)	0.98	2.54	3.379(6)	143
C(24)-H(24C)···O(4)	0.98	2.54	3.346(5)	140

C-H···π interactions

X-H···Cg(J)	H···Cg(J) (Å)	H-Perp[a] (Å)	γ[b] (º)	X···Cg(J) (Å)	X-H, Pi[c] (º)
C(17)-H(17B)···Cg(1)	2.80	2.66	17.78	3.754(5)	72

π···π interactions

Cg(I)···Cg(J)	Cg···Cg[d] (Å)	α[e] (º)	β, γ[f] (º)	$d_{plane-plane}$[g] (Å)	d_{offset}[h] (Å)
Cg(1)···Cg(2)	3.451(3)	5.7(3)	18.8, 17.7	3.2879(17), 3.267(2)	1.114
Cg(2)···Cg(2)	3.366(3)	0.0(3)	3.2	3.360(2)	0.188

[a]Perpendicular distance of H to ring plane J. [b]Angle between Cg(J)-H vector and ring J normal. [c]Angle of the X-H bond with the Pi-plane (Perpendicular = 90º, Parallel = 0º) [d]Cg···Cg = distance between ring centroids; [e]α= dihedral angle between Planes I and J; [f]Offset angles: β = angle Cg(I)-Cg(J) and normal to plane I and γ = angle Cg(I)-Cg(J) and normal to plane J (β = γ, when α = 0º); [g]Perpendicular distance of Cg(I) on plane J and perpendicular distance of Cg(J) on plane I (equal when α = 0º); [h]Slippage = Horizontal displacement or slippage between Cg(I) and Cg(J) (equal for both centroids when α = 0º). Cg(1) = O(2) C(2) C(3) C(4) C(5); Cg(2) = O(6) C(7) C(8) C(9) C(10).

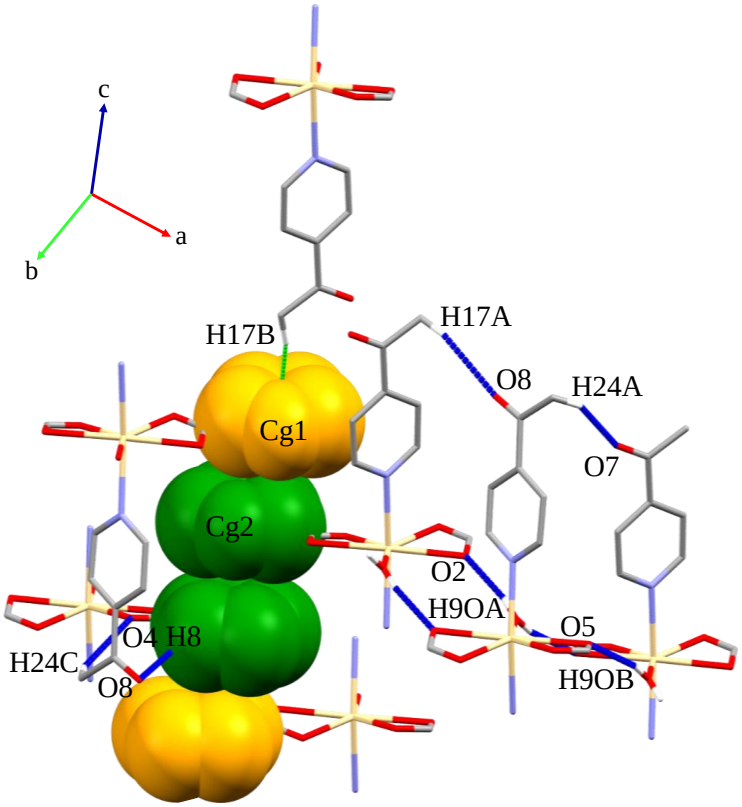

Figure S29. Supramolecular expansion of **4**. Hydrogen atoms have been omitted for clarity.

Compound **5.** The H(8B) atom from a coordinated water molecule in *A* associate with the carbonyl O(15) atom of 4-Acpy, in combination with a π···π interaction (Cg(1)···Cg(2), 3.992(3) Å, Table S5) between 2-FA and 4-Acpy resulting in the pilling of *A* and *B* chains along the [10$\bar{1}$] direction (Fig. S20a). Then, an additional π···π interaction between furane rings (Cg(3)···Cg(4), 3.677 Å) supplements the association of *A* and *B* in parallel along the *b* axis (Fig. S20b). This combination expands the structure forming a 3D net.

Table S5. Intermolecular interactions present in complex **5**.

Intermolecular Interactions		D-H (Å)		H···A	D···A (Å)	>D-H···A
O(7)-H(7A)···O(10)		0.80(3)		1.91(3)	2.710(5)	175(5)
O(8)-H(8B)···O(15)		0.80(3)		2.02(4)	2.767(6)	155(5)
π···π interactions						
Cg(I)···Cg(	Cg···Cg[a]	α[b] (º)	β, γ[c] (º)		$d_{plane-plane}$[d] (Å)	d_{offset}[e] (Å)
Cg(1)···Cg	3.992(3)	23.9(3	34.1,		3.887(2), 3.306(2)	2.238
Cg(3)···Cg	3.676(3)	15.9(3	20.4,		3.591(2), 3.4469(19)	1.279

[a]Cg···Cg = distance between ring centroids; [a]Cg···Cg = distance between ring centroids; [b]α= dihedral angle between Planes I and J; [c]Offset angles: β = angle Cg(I)-Cg(J) and normal to plane I and γ = angle Cg(I)-Cg(J) and normal to plane J (β = γ, when α = 0º); [d]Perpendicular distance of Cg(I) on plane J and perpendicular distance of Cg(J) on plane I (equal when α = 0º); [e]Slippage = Horizontal displacement or slippage between Cg(I) and Cg(J) (equal for both centroids when α = 0º). Cg(1) = O(3) C(2) C(3) C(4) C(5); Cg(2) = N(1) C(21) C(22) C(23) C(24) C(25); Cg(3) = O(6) C(7) C(8) C(9) C(10); Cg(4) = O(14) C(17) C(18) C(19) C(20).

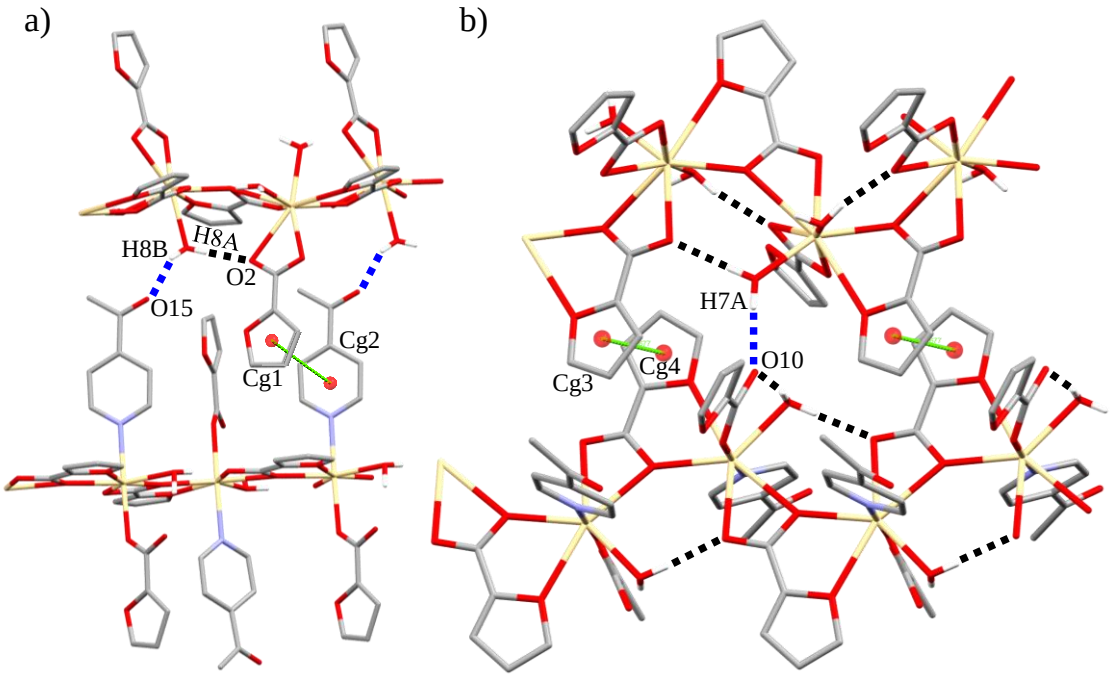

Figure S30. (a) Representation of the intermolecular interactions (blue dashed lines) of **5** assembling A and B chains. (b) Intramolecular interactions are intended to further differentiation. Hydrogen atoms not involved in the associations have been omitted for clarity.

Photophysical properties

UV-Vis spectroscopy

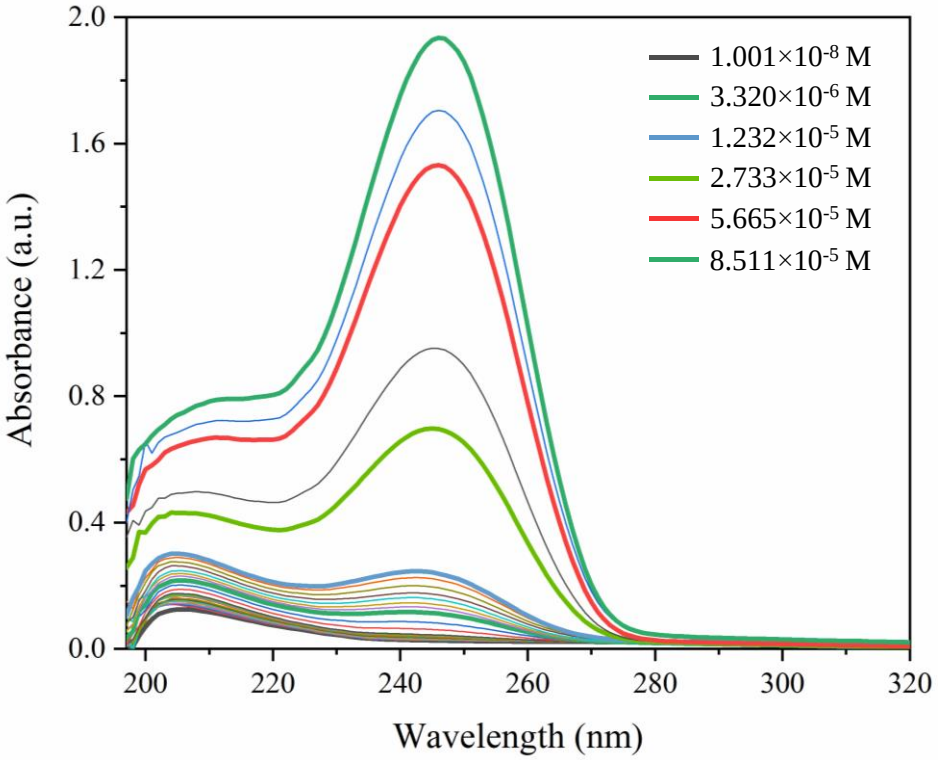

Figure S31. UV-Vis spectrum of 2-furoic acid (2-FA) in MeOH at concentrations between 1.001×10^{-8} M and 8.511×10^{-5} M.

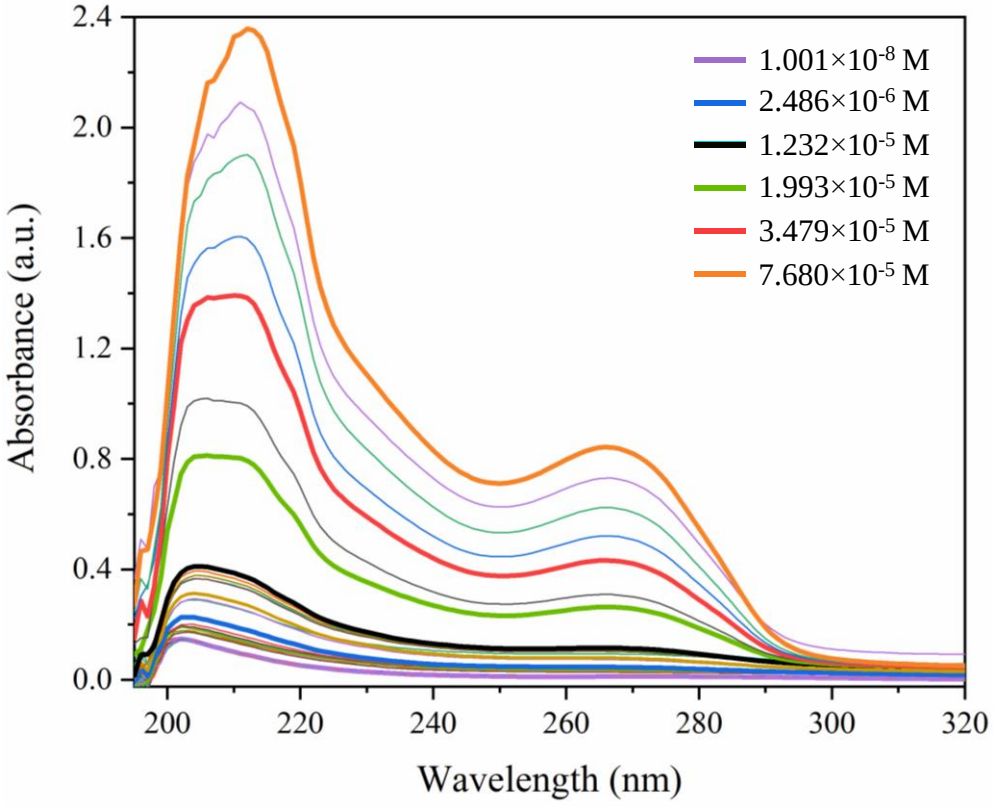

Figure S32. UV-Vis spectrum of isonicotinamide (Isn) in MeOH at concentrations between 1.001×10^{-8} M and 7.680×10^{-5} M.

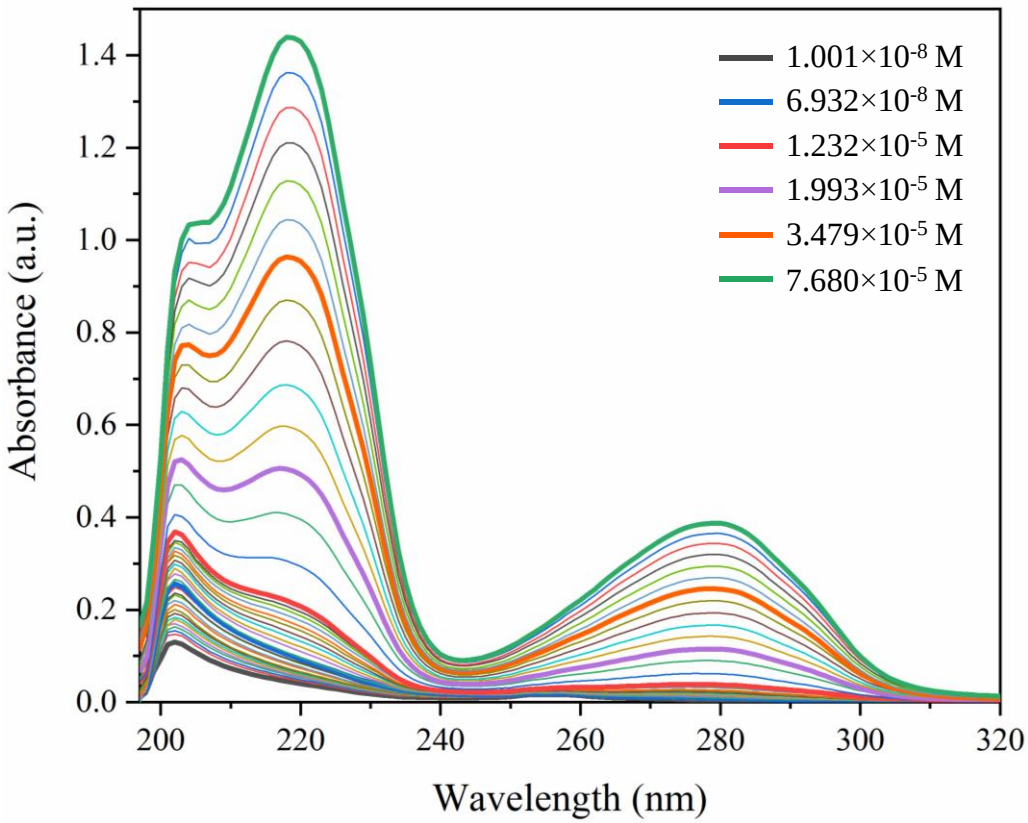

Figure S33. UV-Vis spectrum of 4-acetylpyridine (4-Acpy) in MeOH at concentrations between 1.001×10^{-8} M and 7.680×10^{-5} M.

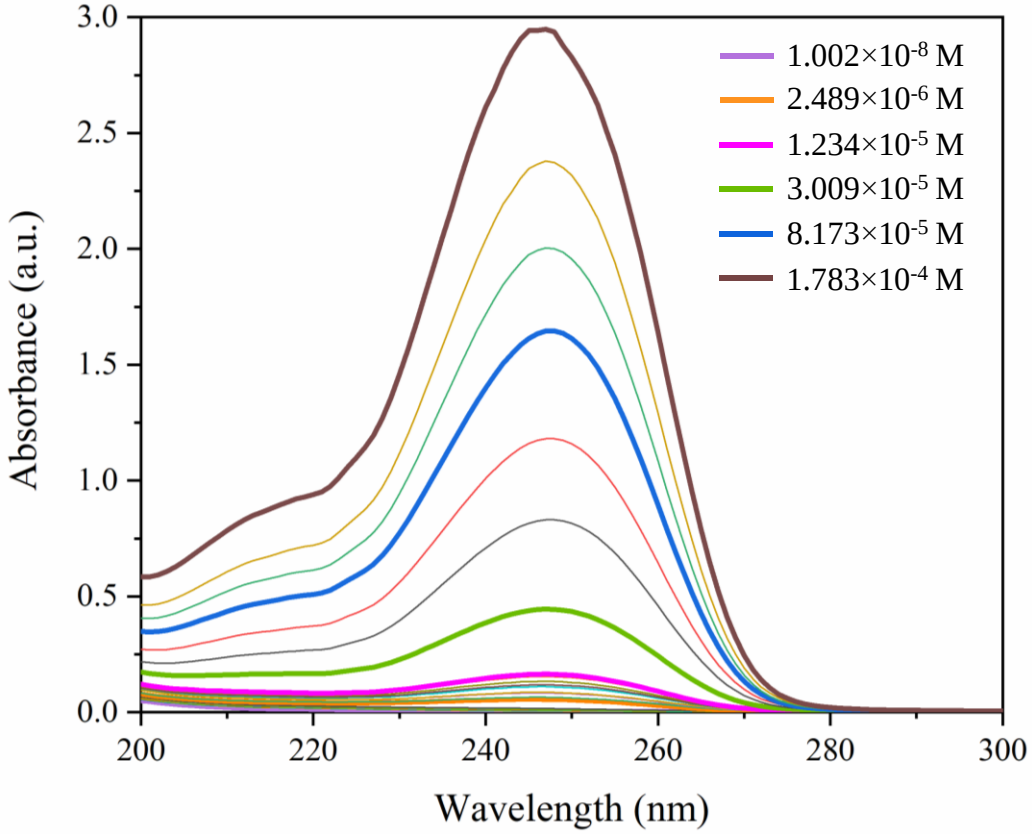

Figure S34. UV-Vis spectrum of 2-furoic acid (2-FA) in ACN at concentrations between 1.002×10^{-8} M and 1.783×10^{-4} M.

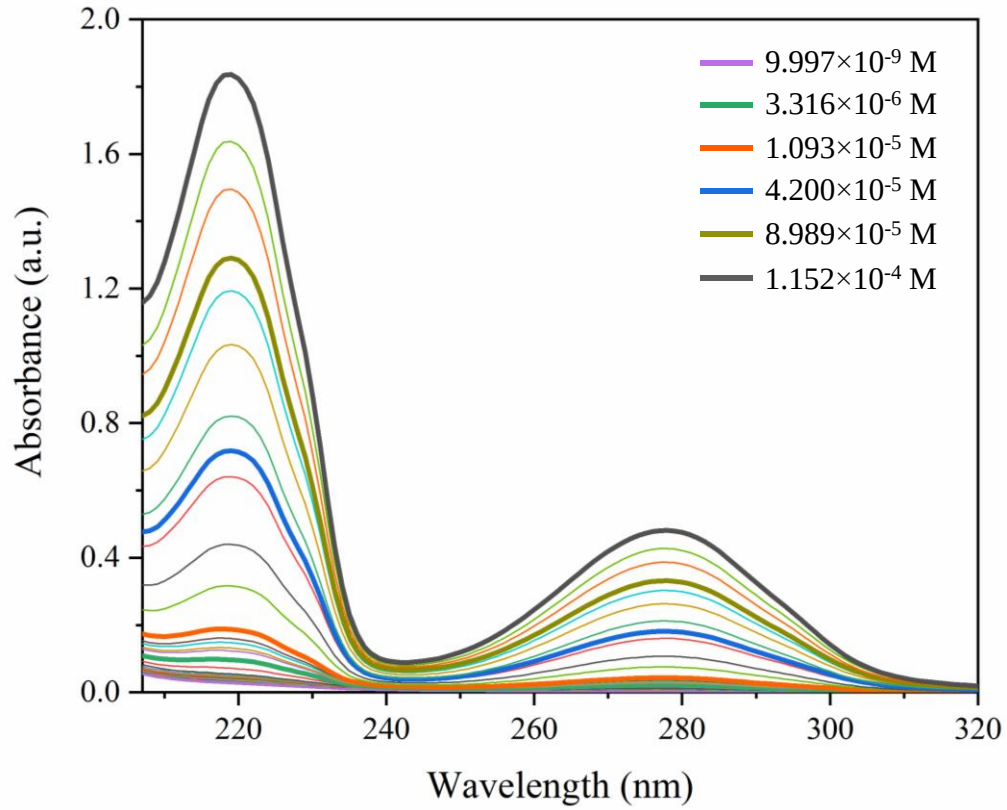

Figure S35. UV-Vis spectrum of 4-acetylpyridine (4-Acpy) in ACN at concentrations between 9.997×10^{-9} M and 1.152×10^{-4} M.

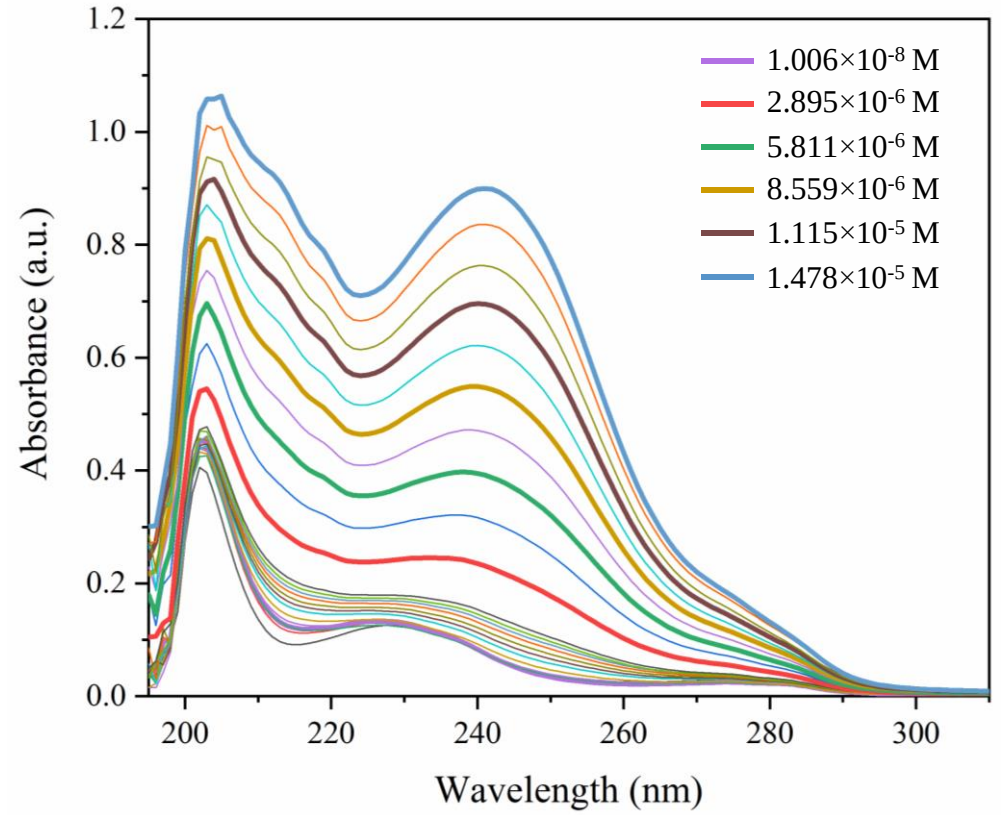

Figure S36. UV-Vis spectrum of $[Zn(\mu\text{-}2\text{-FA})(2\text{-FA})(Isn)_2]_2$ (**1**) in MeOH at concentrations between 1.006×10^{-9} M and 1.478×10^{-5} M.

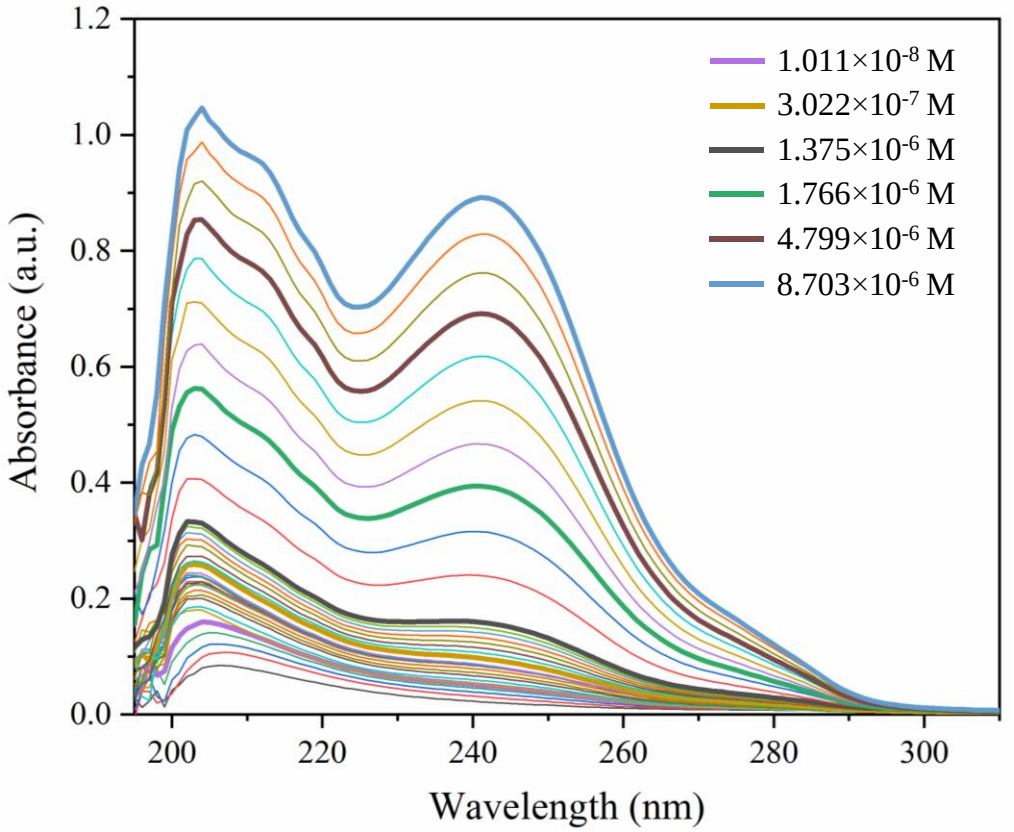

Figure S37. UV-Vis spectrum of $[Cd(\mu\text{-}2\text{-}FA)(2\text{-}FA)(Isn)_2]_2$ (**2**) in MeOH at concentrations between 1.011×10^{-9} M and 8.703×10^{-6} M.

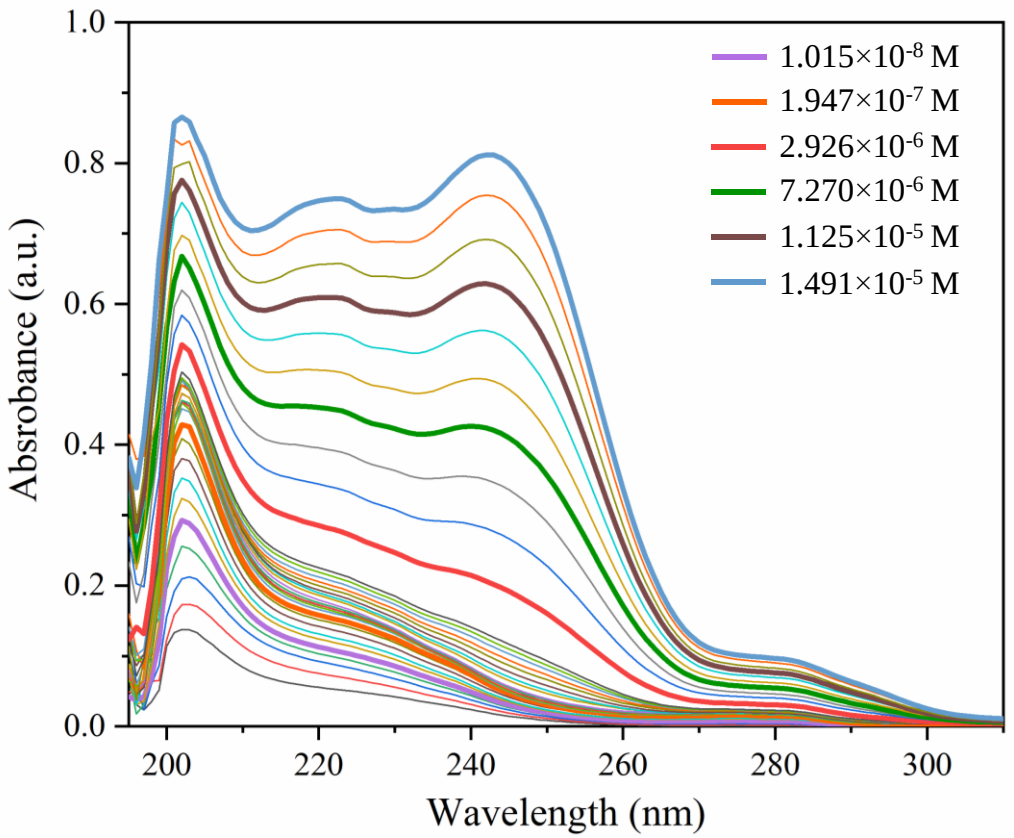

Figure S38. UV-Vis spectrum of $[Zn(\mu\text{-}2\text{-}FA)_2(4\text{-}Acpy)]_2$ (**3**) in MeOH at concentrations between 1.015×10^{-9} M and 1.491×10^{-5} M.

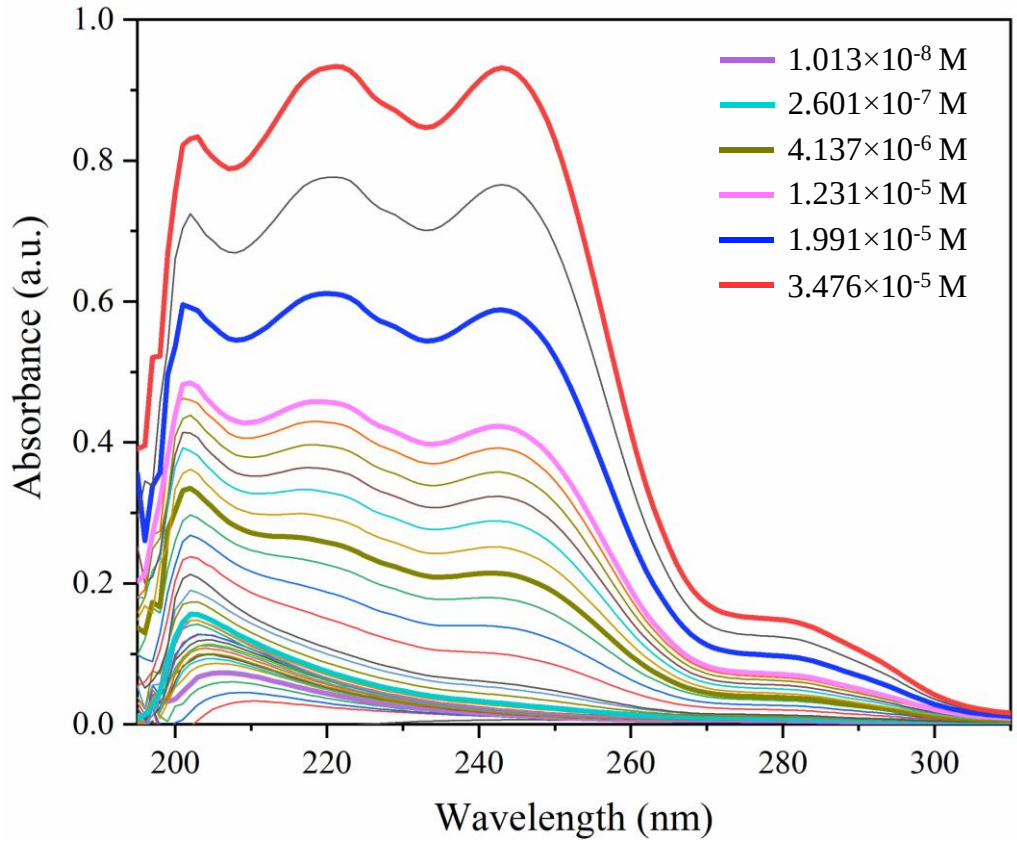

Figure S39. UV-Vis spectrum of $[Cd(2\text{-}FA)_2(4\text{-}Acpy)_2(OH_2)]$ (**4**) in MeOH at concentrations between 1.014×10^{-9} M and 3.476×10^{-5} M.

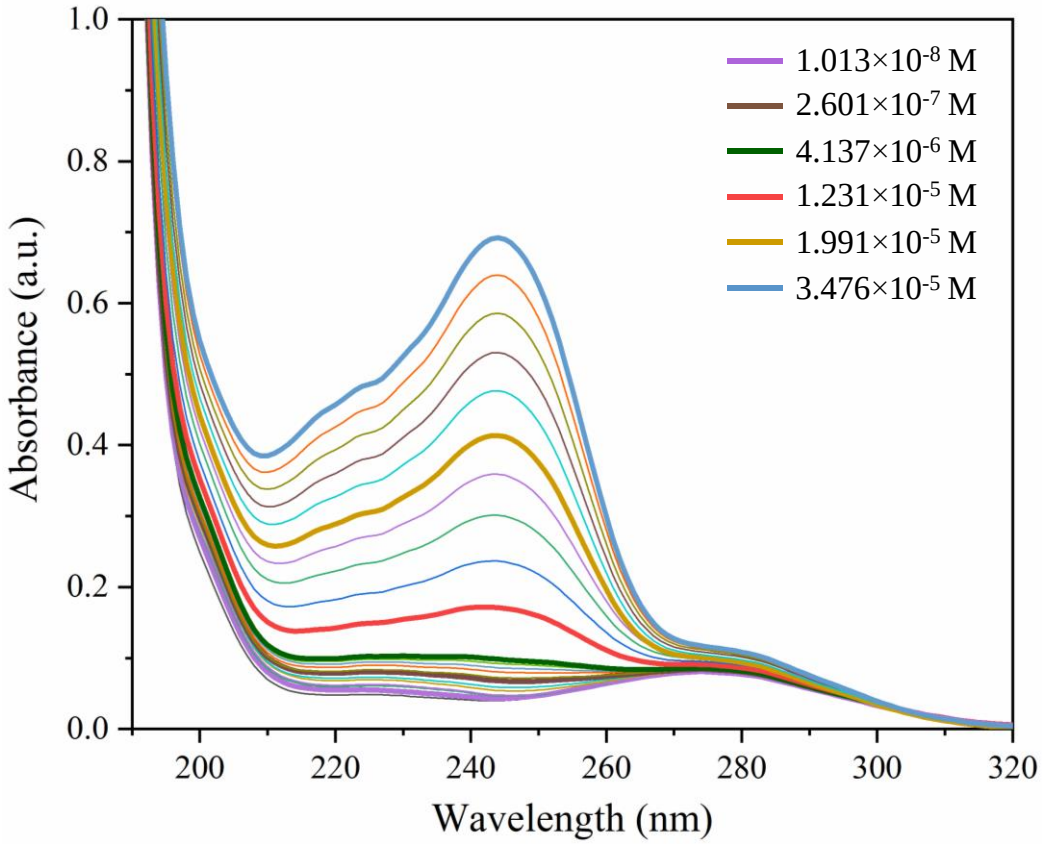

Figure S40. UV-Vis spectrum of $\{[Cd(\mu\text{-}2\text{-}FA)_2(OH_2)_2]_n[Cd(\mu\text{-}2\text{-}FA)_2(4\text{-}Acpy)(OH_2)]_n\}$ (**5**) in ACN at concentrations between 1.000×10^{-9} M and 1.232×10^{-5} M.

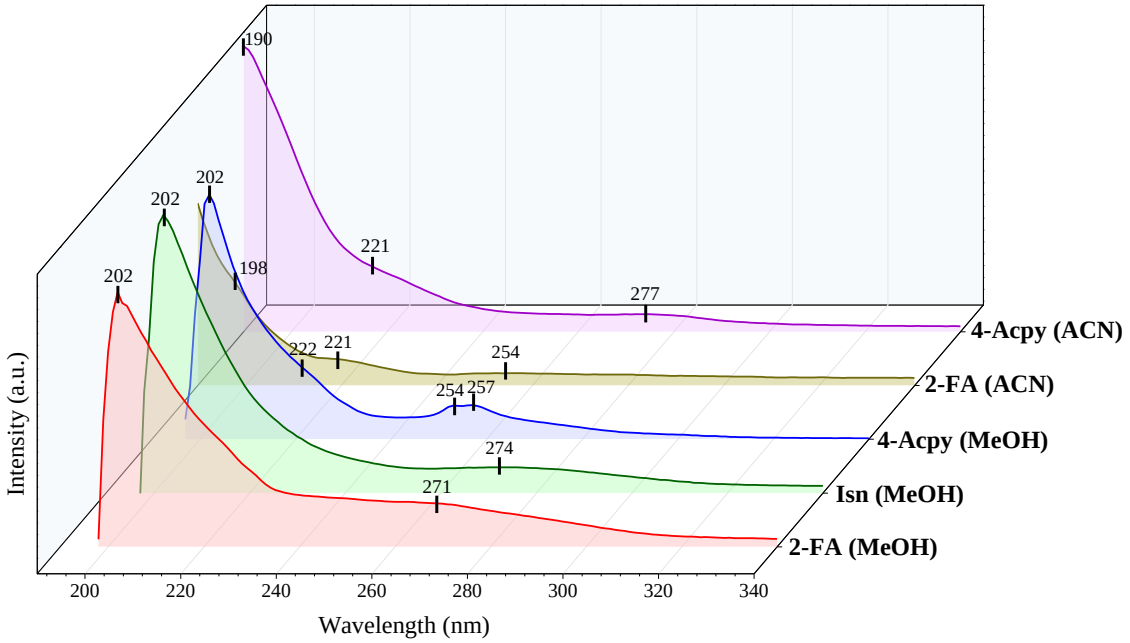

Figure S41. UV-Vis spectra of 2-FA (in MeOH and ACN), Isn (in MeOH) and 4-Acpy (in MeOH and ACN) at a concentration of 1.001×10^{-8} M (2-FA in MeOH), 1.001×10^{-8} M (Isn in MeOH), 1.001×10^{-8} M (4-Acpy in MeOH), 1.002×10^{-8} M (2-FA in ACN), and 9.997×10^{-9} M (4-Acpy in ACN).

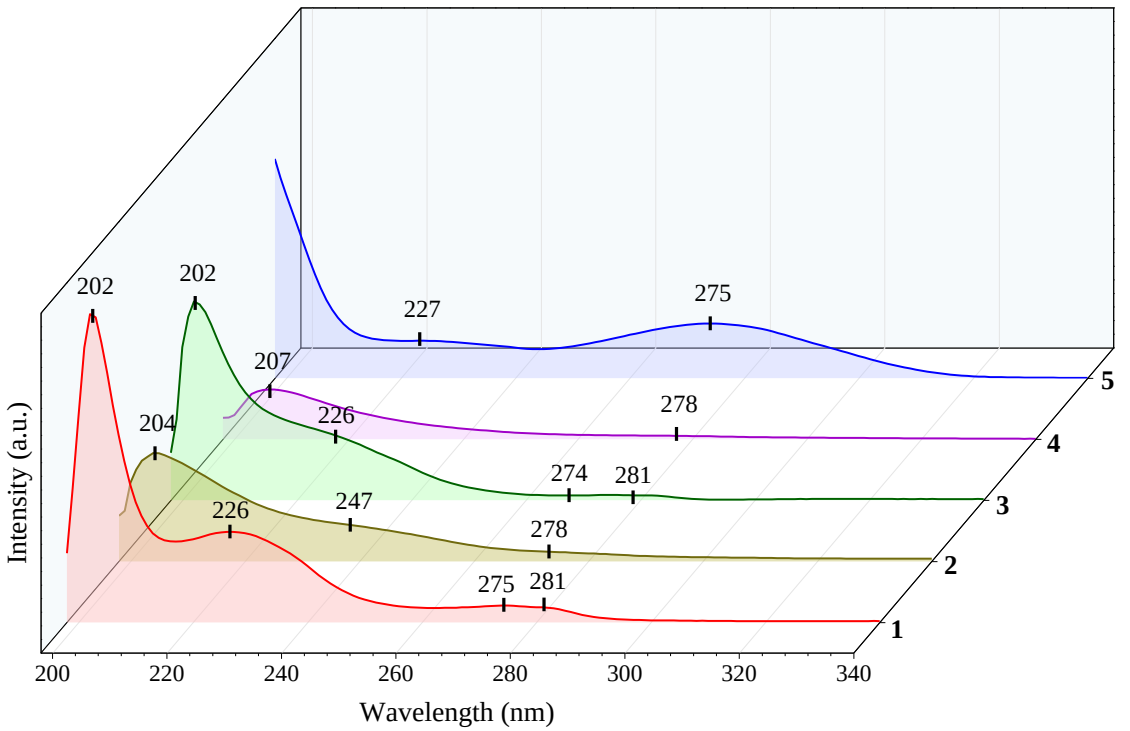

Figure S42. UV-Vis spectra of complexes **1**-**4** (in MeOH), and **5** (in ACN) at a concentration of 1.006×10^{-8} M (**1**), 1.011×10^{-8} M (**2**), 1.015×10^{-8} M (**3**), 1.013×10^{-8} M (**4**), 1.000×10^{-8} M (**5**).

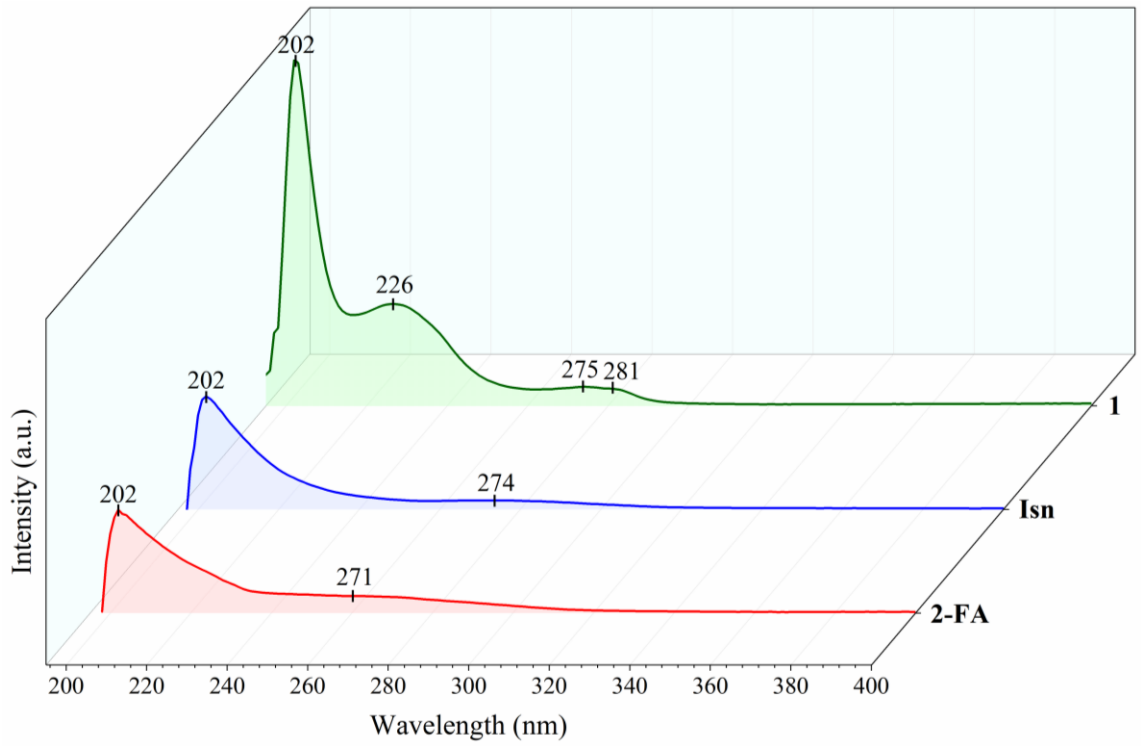

Figure S43. UV-Vis spectra of **1** and their corresponding ligands (2-FA and Isn) using 1.001×10^{-8} M (2-FA), 1.001×10^{-8} M (Isn), and 1.006×10^{-8} M (**1**) solutions in MeOH.

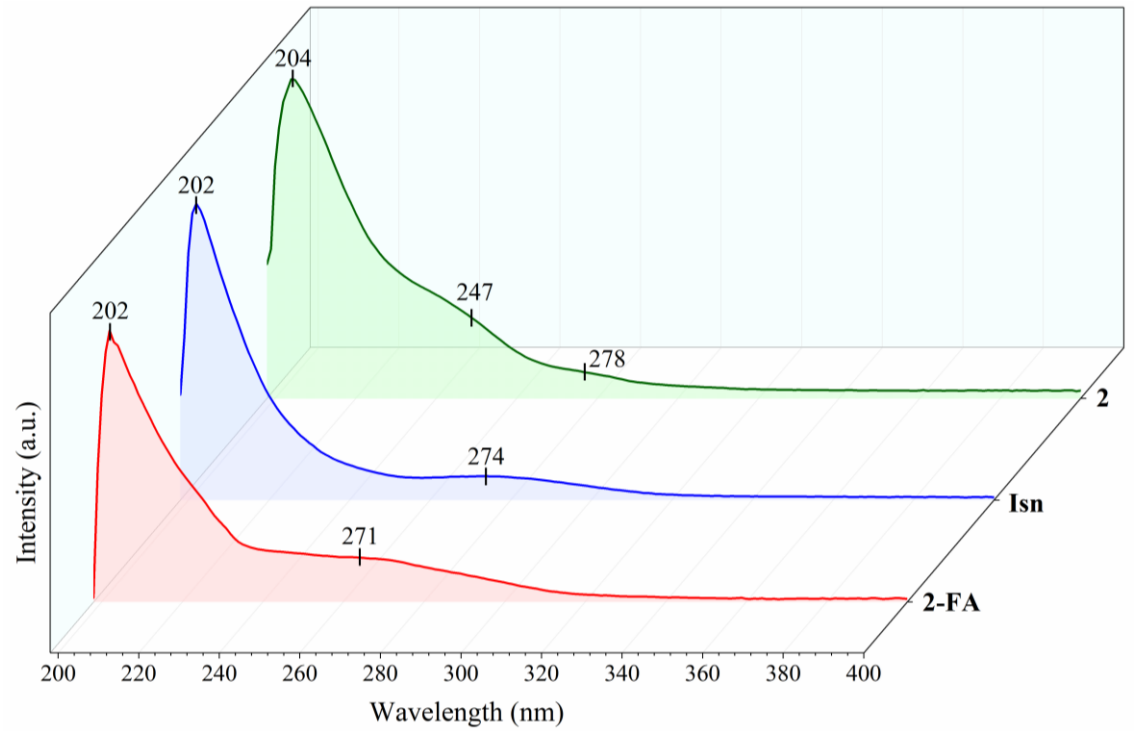

Figure S44. UV-Vis spectra of **2** and their corresponding ligands (2-FA and Isn) using 1.001×10^{-8} M (2-FA), 1.001×10^{-8} M (Isn), and 1.011×10^{-8} M (**2**) solutions in MeOH.

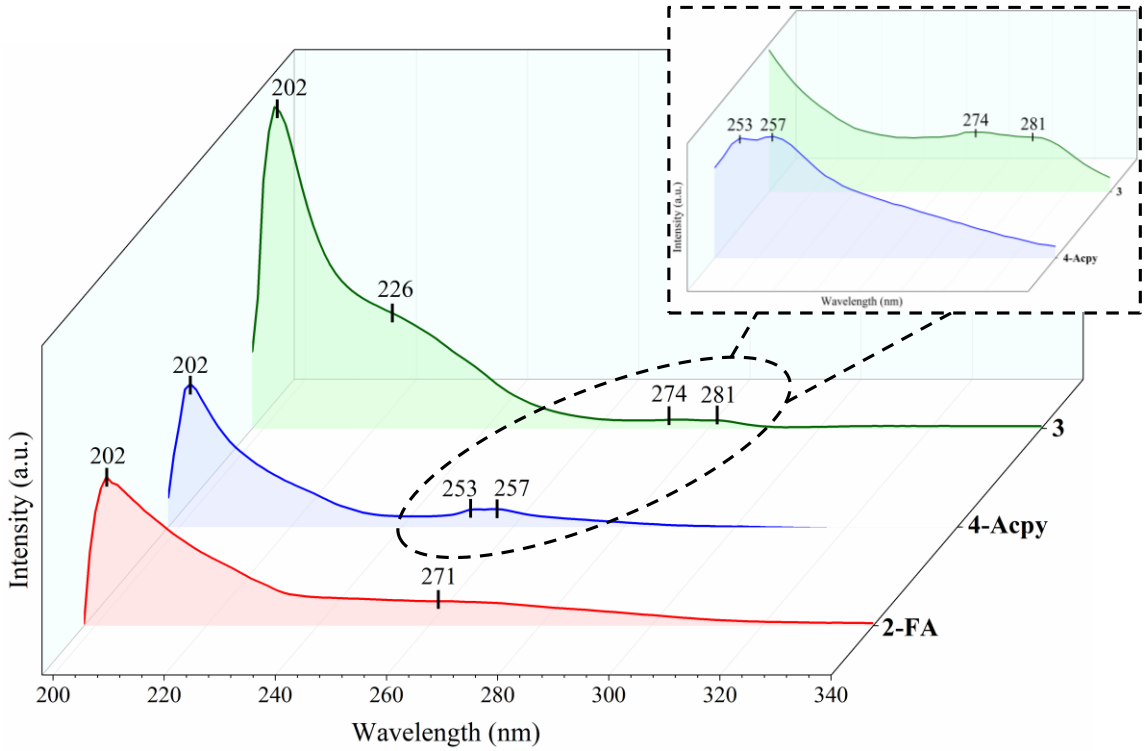

Figure S45. UV-Vis spectra of **3** and their corresponding ligands (2-FA and 4-Acpy) using 1.001×10^{-8} M (2-FA), 1.001×10^{-8} M (4-Acpy), and 1.015×10^{-8} M (**3**) solutions in MeOH.

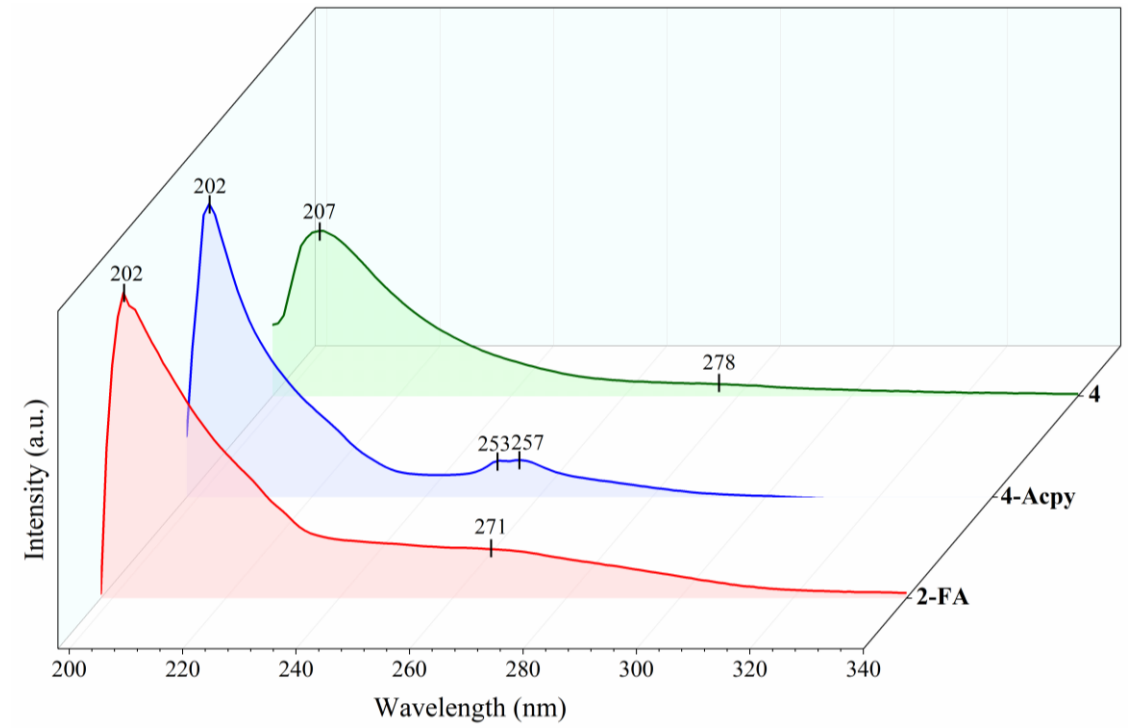

Figure S46. UV-Vis spectra of **4** and their corresponding ligands (2-FA and 4-Acpy) using 1.001×10^{-8} M (2-FA), 1.001×10^{-8} M (4-Acpy), and 1.013×10^{-8} M (**4**) solutions in MeOH.

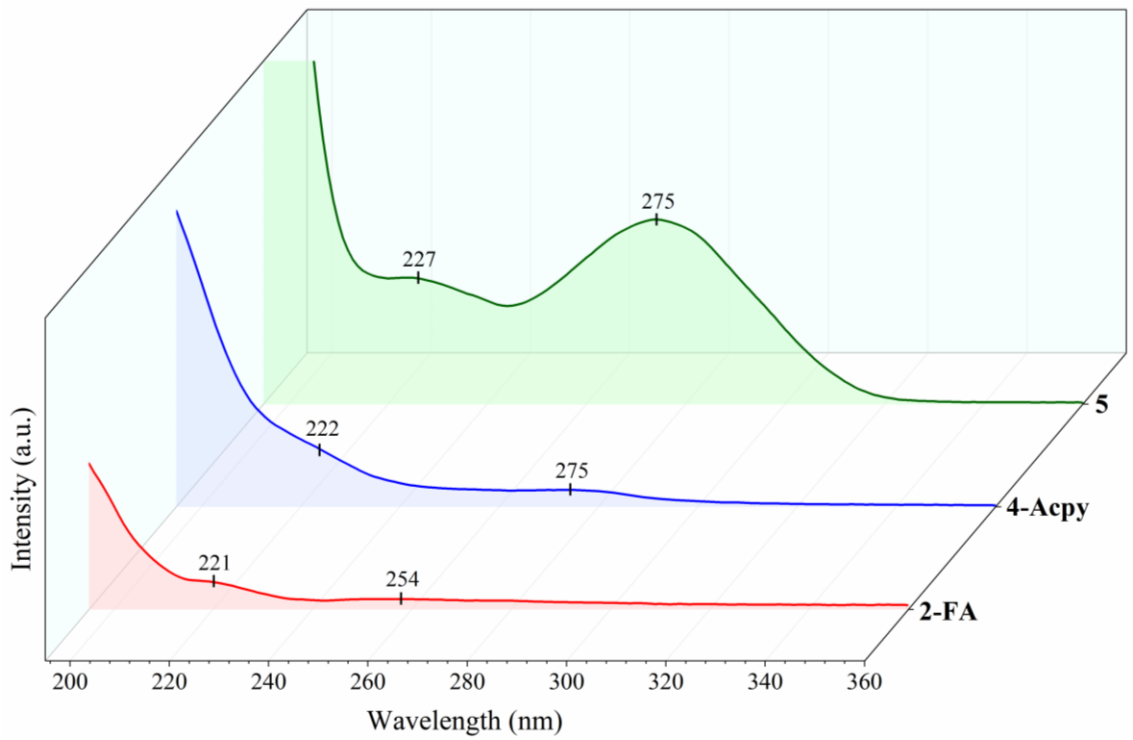

Figure S47. UV-Vis spectra of **5** and their corresponding ligands (2-FA and 4-Acpy) using 1.002×10^{-8} M (2-FA), 9.997×10^{-9} M (4-Acpy), and 1.000×10^{-8} M (**5**) solutions in ACN.

Fluorescence

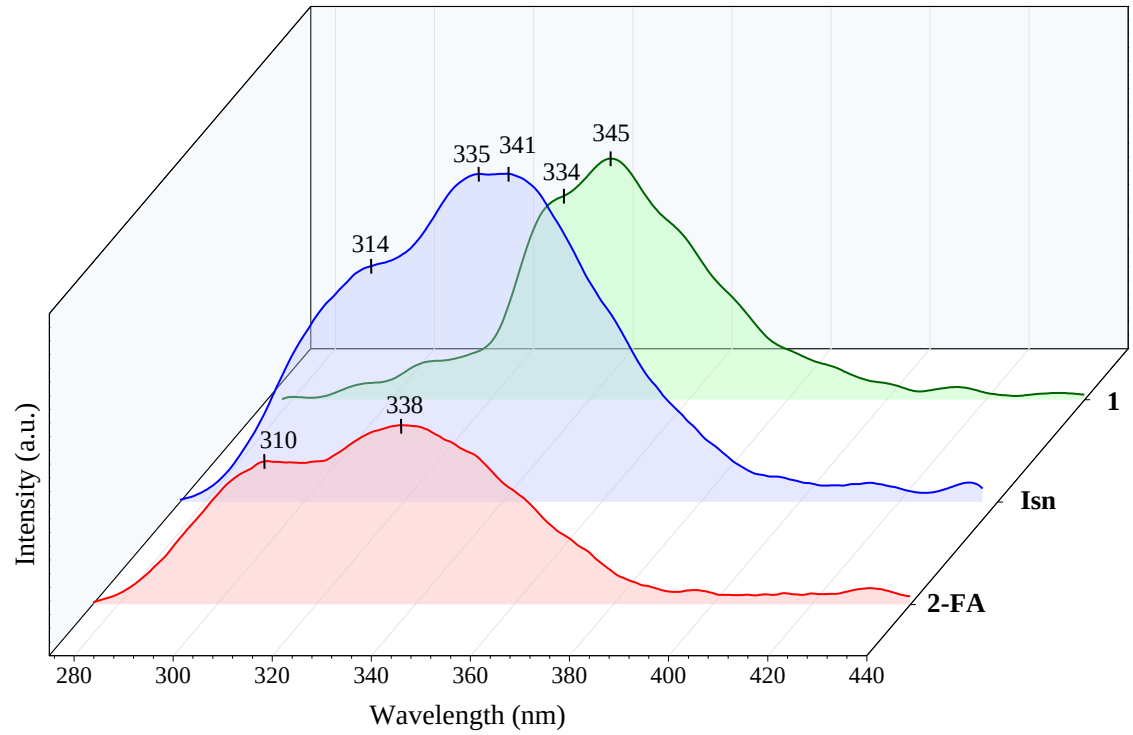

Figure S48. Emission spectra of **1** and their corresponding ligands (2-FA and Isn) irradiated at 227 nm using 1.001×10^{-8} M (2-FA), 1.001×10^{-8} M (Isn), and 1.006×10^{-8} M (**1**) solutions in MeOH.

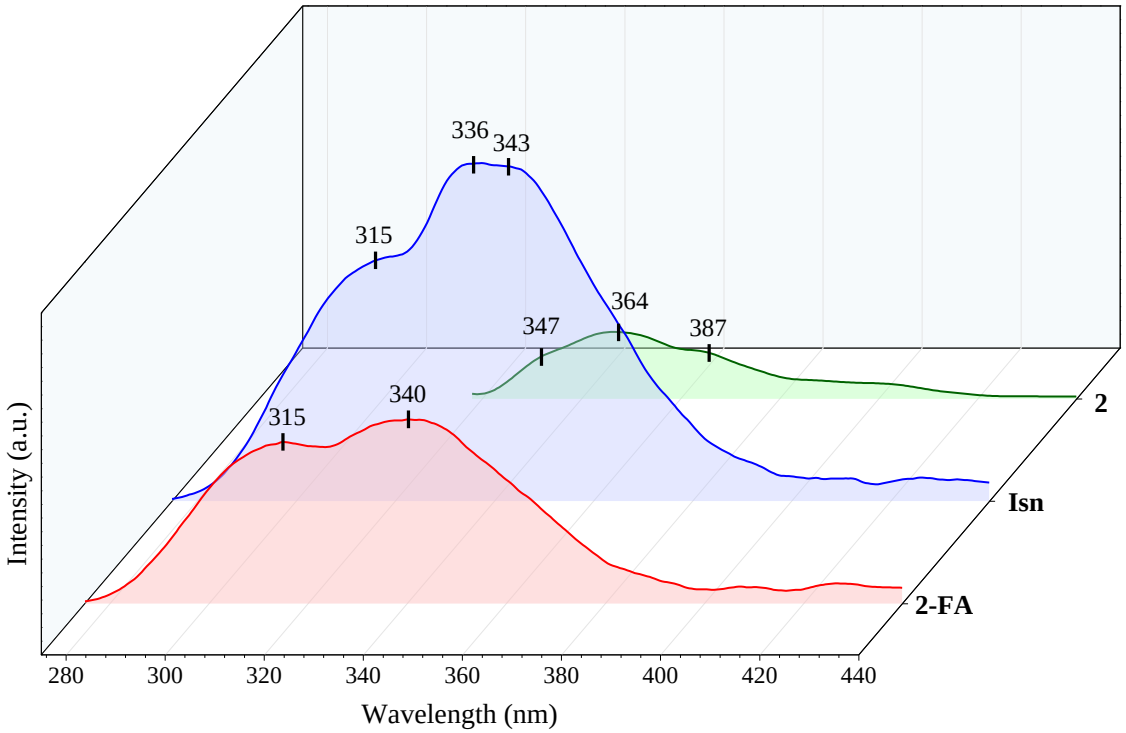

Figure S49. Emission spectra of **2** and their corresponding ligands (2-FA and Isn) irradiated at 230 nm using 1.001×10^{-8} M (2-FA), 1.001×10^{-8} M (Isn), and 1.011×10^{-8} M (**2**) solutions in MeOH.

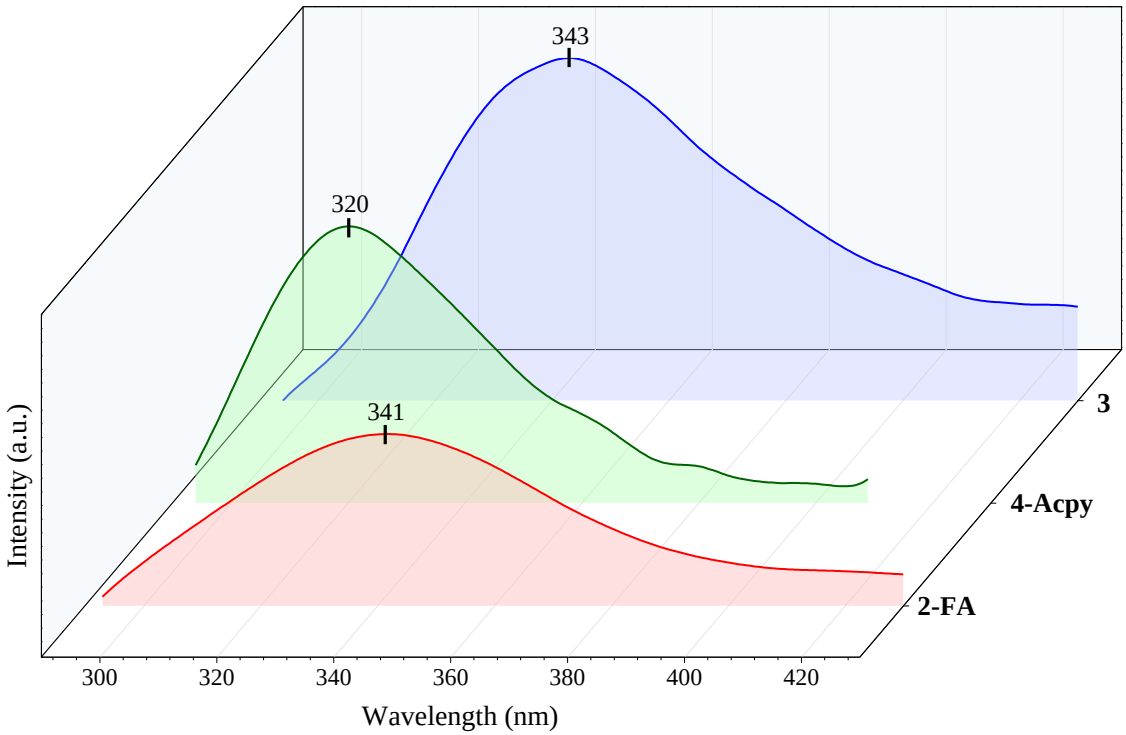

Figure S50. Emission spectra of **3** and their corresponding ligands (2-FA and 4-Acpy) irradiated at 281 nm using 1.001×10^{-8} M (2-FA), 1.001×10^{-8} M (4-Acpy), and 1.015×10^{-8} M (**3**) solutions in MeOH.

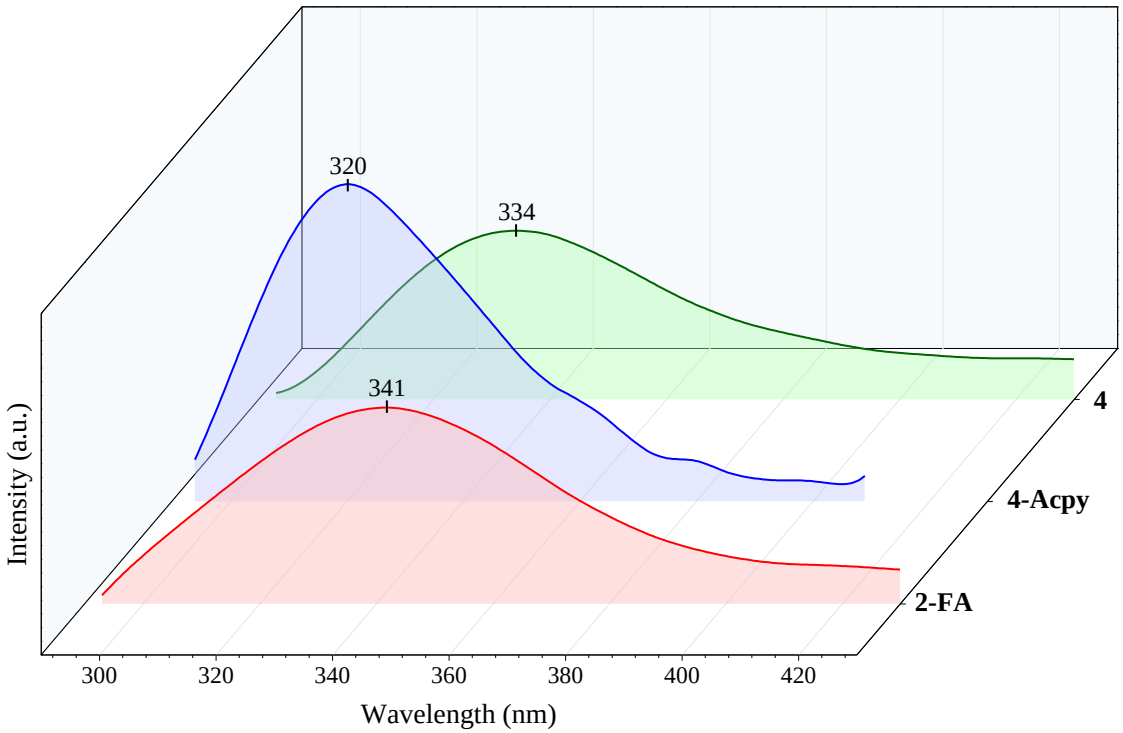

Figure S51. Emission spectra of **4** and their corresponding ligands (2-FA and 4-Acpy) irradiated at 281 nm using 1.001×10^{-8} M (2-FA), 1.001×10^{-8} M (4-Acpy), and 1.013×10^{-8} M (**4**) solutions in MeOH.

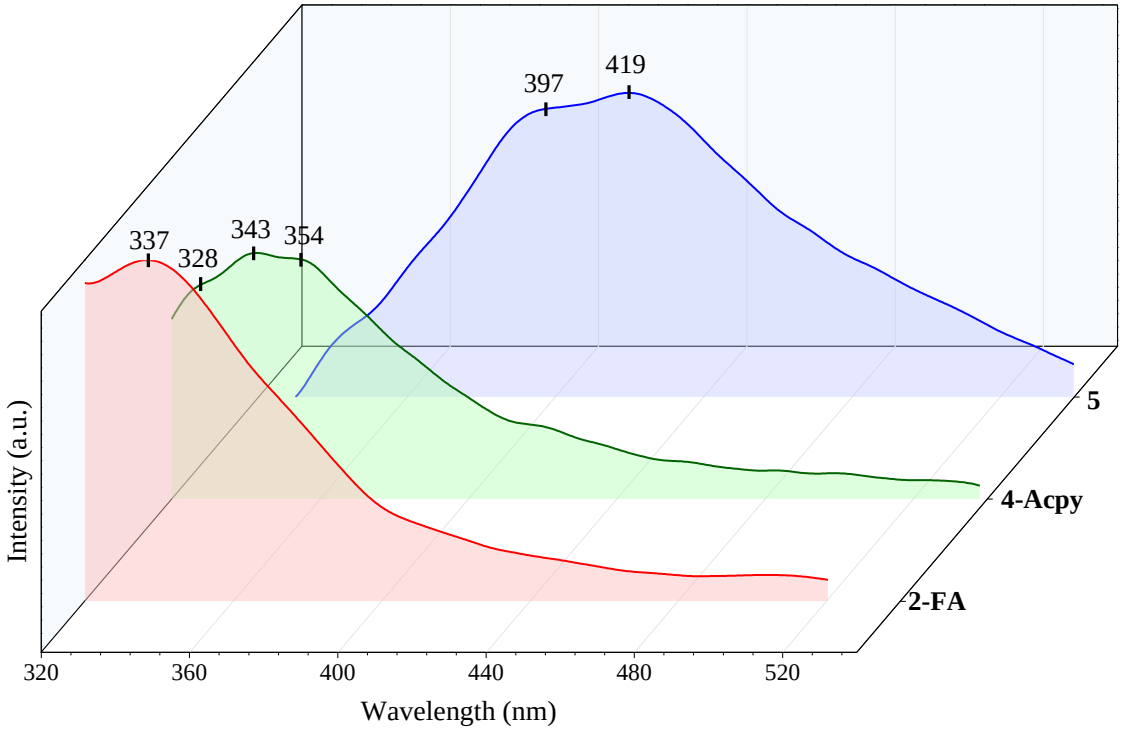

Figure S52. Emission spectra of **5** and their corresponding ligands (2-FA and 4-Acpy) irradiated at 281 nm using 1.002×10^{-8} M (2-FA), 9.997×10^{-9} M (4-Acpy), and 1.000×10^{-8} M (**5**) solutions in ACN.

Table S6. Relevant parameters of the photophysical properties of the ligands[a].

Ligand	Solvent	$\lambda_{max\text{-}abs}$ (log(ε))	λ_{exc}	$\lambda_{max\text{-}em}$	Stokes shift
2-FA	MeOH	202 (3.85), 271 (3.24)	227	310, 338	11795, 14467
			230	315, 340	11732, 14066
			281	341	6262
	ACN	190* (3.63), 198 (3.50), 221 (4.21), 254 (4.07)	281	337	5914
Isn	MeOH	202 (4.43), 274 (4.02)	227	314, 335, 341	12206, 14202, 14727
			230	315, 336, 343	11732, 13716, 14324
4-Acpy	MeOH	202 (4.08), 222 (4.15), 254, 257	281	320	4337
	ACN	190 (5.05), 217 (4.16), 277 (3.59) (3.58)	281	328, 343, 354, 418	5099, 6433, 7339, 11664

*Absorption maxima is out of range and the data of the highest energy peak is provided. [a]All the wavelengths are given in nm. ε values are given in $M^{-1}\times cm^{-1}$. Stokes shift values are given in cm^{-1}. $\lambda_{max\text{-}abs}$ = maximum of absorption; λ_{exc} = excitation maximum; $\lambda_{max\text{-}em}$ = maximum of emission.

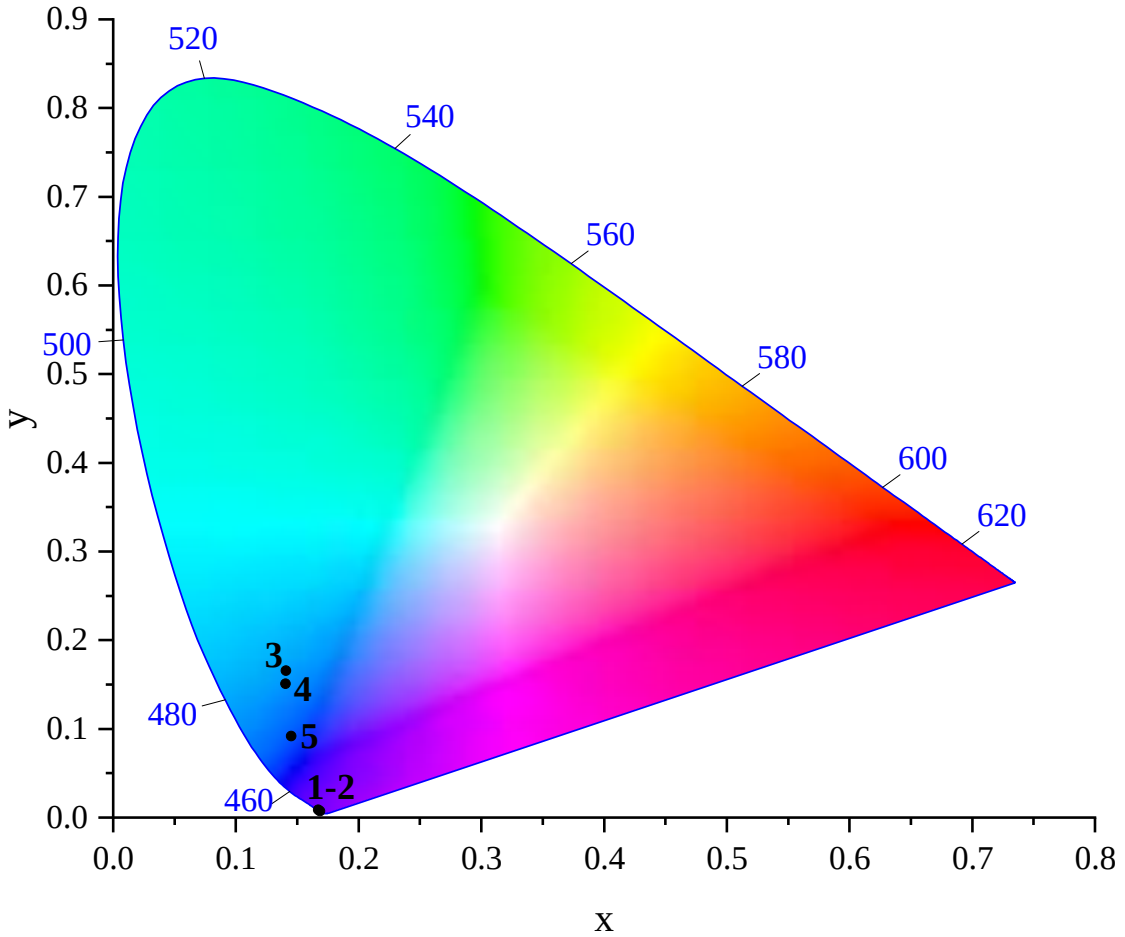

Figure S53. CIE 1931 chromaticity diagram for **1-5**.

References

1 M. Llunell, D. Casanova, J. Cirera, P. Alemany and S. Alvarez. *SHAPE. Program for the Stereochemical Analysis of Molecular Fragments by Means of Continuous Shape Measures and Associated Tools*. Universitat de Barcelona, Barcelona 2013.

2 M. Pinsky and D. Avnir, *Inorg. Chem.*, 1998, **37**, 5575–5582.